

A multi-resolution approximation via linear projection for large spatial datasets

Toshihiro Hirano

Kanto Gakuin University

Abstract

Recent technical advances in collecting spatial data have been increasing the demand for methods to analyze large spatial datasets. The statistical analysis for these types of datasets can provide useful knowledge in various fields. However, conventional spatial statistical methods, such as maximum likelihood estimation and kriging, are impractically time-consuming for large spatial datasets due to the necessary matrix inversions. To cope with this problem, we propose a multi-resolution approximation via linear projection (M -RA-lp). The M -RA-lp conducts a linear projection approach on each subregion whenever a spatial domain is subdivided, which leads to an approximated covariance function capturing both the large- and small-scale spatial variations. Moreover, we elicit the algorithms for fast computation of the log-likelihood function and predictive distribution with the approximated covariance function obtained by the M -RA-lp. Simulation studies and a real data analysis for air dose rates demonstrate that our proposed M -RA-lp works well relative to the related existing methods.

Keywords: Covariance tapering; Gaussian process; Geostatistics; Large spatial datasets; Multi-resolution approximation; Stochastic matrix approximation

1 Introduction

Advances in Global Navigation Satellite System (GNSS) and compact sensing devices have made it easy to collect a large volume of spatial data with coordinates in various fields such as environmental science, traffic, and urban engineering. The statistical analysis for these types of spatial datasets would assist in an evidence-based environmental policy and the efficient management of a smart city.

In spatial statistics, this type of statistical analysis, including model fitting and spatial prediction, has been conducted based on Gaussian processes (see, e.g., Cressie and Wikle, 2011). However, traditional spatial statistical methods, such as maximum likelihood

E-mail: 1hirano2@kanto-gakuin.ac.jp

estimation and kriging, are computationally infeasible for large spatial datasets, requiring $O(n^3)$ operations for a dataset of size n . This is because these methods involve the inversion of an $n \times n$ covariance matrix.

This difficulty has encouraged the development of many efficient statistical techniques for large spatial datasets. Heaton et al. (2019) comprehensively reviews recent developments of these techniques. Liu et al. (2020) is a detailed survey on current state-of-the-art scalable Gaussian processes in the machine learning literature. Efficient statistical techniques are generally categorized into four types: a sparse approach, a low rank approach, a spectral approach, and an algorithmic approach. The main idea of the sparse approach is to model either the covariance matrix or its inverse matrix as a sparse matrix. The former method is typically called covariance tapering (Furrer et al., 2006; Kaufman et al., 2008). Du et al. (2009), Chu et al. (2011), Wang and Loh (2011), Hirano and Yajima (2013), Stein (2013), and Furrer et al. (2016) discussed further statistical properties of the covariance tapering. However, the covariance tapering ignores the large-scale spatial variation. The latter one includes the approximation of the likelihood function by using products of the lower-dimensional conditional distributions (e.g., Vecchia, 1988; Stein et al., 2004), an approximation by the Gaussian Markov random field by using a particular type of stochastic partial differential equation (Lindgren et al., 2011), the representation of a field by using a multiresolution basis (Nychka et al., 2015), and the nearest-neighbor Gaussian process by using a directed acyclic graph (Datta et al., 2016).

The low rank approach includes the following two techniques: fixed rank kriging (Cressie and Johannesson, 2008) and predictive process (Banerjee et al., 2008). Finley et al. (2009) corrected a bias in the predictive process, and Banerjee et al. (2013) proposed a linear projection approach that is an extension of the predictive process and has the advantage of alleviating the complicated knot selection problem. However, the predictive process and the linear projection are effective for fitting the large-scale spatial variation, whereas they are disadvantageous for capturing the small-scale spatial variation. To overcome this problem, Sang and Huang (2012) and Katzfuss (2017) developed improvements of the predictive process, and Hirano (2017) proposed a modification of the linear projection by the covariance tapering based on the idea of Sang and Huang (2012).

For the spectral approach, Fuentes (2007), Matsuda and Yajima (2009), and Matsuda and Yajima (2018) considered the Whittle estimation for either spatial or spatio-temporal data. The Whittle estimation requires no huge matrix inversions. Fuentes (2007), Matsuda and Yajima (2009), and Matsuda and Yajima (2018) revealed the statistical properties of the estimation by the spectral approach. Guinness (2019) developed a computationally efficient method for estimating the spectral density from incomplete

gridded data based on imputing missing values.

The algorithmic approach focuses more on using schemes than model building and includes Gramacy and Apley (2015), Gerber et al. (2018), and Guhaniyogi and Banerjee (2018).

In this paper, we propose a multi-resolution approximation via linear projection (M -RA-lp) of Gaussian processes observed at irregularly spaced locations. The M -RA-lp implements the linear projection on each subregion obtained by partitioning the spatial domain recursively, resulting in an approximated covariance function that captures both the large- and small-scale spatial variations unlike the covariance tapering and some low rank approaches. Additionally, we derive algorithms for fast computation of the log-likelihood function and predictive distribution with the approximated covariance function obtained by the M -RA-lp. Also, these algorithms can be parallelized. Our proposed M -RA-lp is regarded as a combination of the two recent low rank approaches: a modified linear projection (MLP) (Hirano, 2017) and a multi-resolution approximation (M -RA) (Katzfuss, 2017). The M -RA-lp extends the MLP by introducing multiple resolutions based on the idea of Katzfuss (2017), leading to better approximation accuracy of the covariance function than that by the MLP. Particularly, when the variation of the spatial correlation around the origin is smooth like the Gaussian covariance function, the approximation accuracy of the covariance function by the MLP often degrades. In contrast, the M -RA-lp avoids this problem. Additionally, the M -RA-lp is regarded as an extension of the M -RA and enables not only to alleviate the knot selection problem but also to increase empirically numerical stability in specific steps of fast computation algorithms of the M -RA. Simulation studies and a real data analysis for air dose rates generally support the effectiveness of our proposed M -RA-lp in terms of computational time, estimation of model parameters, and prediction at unobserved locations when compared with the MLP and M -RA.

The remainder of this paper is organized as follows. We introduce a Gaussian process model for spatial datasets in Section 2. Section 3 describes our proposed M -RA-lp. In Section 4, we present the algorithms for fast computation of the log-likelihood function and predictive distribution. In Section 5, we provide the results of the simulation studies and real data analysis. Our conclusions and future studies are discussed in Section 6. The appendices contain technical lemmas, the proof of the proposition, and the derivation and distributed computing of the algorithms.

2 Gaussian process model for spatial datasets

For $\mathbf{s} = (s_1, \dots, s_d)^\top \in D_0 \subset \mathbb{R}^d$ ($d \in \mathbb{N}^+$), we consider the following model

$$Z(\mathbf{s}) = Y_0(\mathbf{s}) + \varepsilon(\mathbf{s}),$$

where $Z(\mathbf{s})$ is a response variable observed at location \mathbf{s} . $Y_0(\mathbf{s}) \sim \text{GP}(0, C_0)$ is a zero-mean Gaussian process with a covariance function $C_0(\mathbf{s}, \mathbf{s}^*)$ ($\mathbf{s}, \mathbf{s}^* \in D_0$), which is a positive definite function. $C_0(\mathbf{s}, \mathbf{s}^*)$ is specified as $\sigma^2 \rho_0(\mathbf{s}, \mathbf{s}^*; \boldsymbol{\theta})$ where $\sigma^2 = \text{Var}(Y_0(\mathbf{s}))$, and ρ_0 means a correlation function of $Y_0(\mathbf{s})$ with a parameter vector $\boldsymbol{\theta}$. For example, $\boldsymbol{\theta}$ may include a range parameter. $\varepsilon(\mathbf{s})$ is a zero-mean independent process following a normal distribution with a variance τ^2 and expresses a measurement error that is often referred to as a nugget effect (see, e.g., Cressie, 1993). It is assumed that $\{Y_0(\mathbf{s})\}$ and $\{\varepsilon(\mathbf{s})\}$ are independent.

In what follows, for a generic Gaussian process $X(\mathbf{s}) \sim \text{GP}(0, C)$ and sets of the vectors, that is, $A = \{\mathbf{a}_1, \dots, \mathbf{a}_N\}$ and $B = \{\mathbf{b}_1, \dots, \mathbf{b}_M\}$ ($\mathbf{a}_i, \mathbf{b}_j \in \mathbb{R}^{d'}$, $i = 1, \dots, N$, $j = 1, \dots, M$), we write $\mathbf{X}(A) = (X(\mathbf{a}_1), \dots, X(\mathbf{a}_N))^\top$ and $(C(A, B))_{ij} = C(\mathbf{a}_i, \mathbf{b}_j)$ ($i = 1, \dots, N$, $j = 1, \dots, M$).

Suppose that we observe the response variable $Z(\mathbf{s})$ at a set of n spatial locations $S_0 = \{\mathbf{s}_1, \dots, \mathbf{s}_n\}$. The observation vector is denoted by $\mathbf{Z}(S_0) = (Z(\mathbf{s}_1), \dots, Z(\mathbf{s}_n))^\top$. The major goal in the spatial statistical analysis is to estimate the parameters $\Omega = (\sigma^2, \boldsymbol{\theta}, \tau^2)$ and to predict $\mathbf{Y}_0(S_0^P) = (Y_0(\mathbf{s}_1^P), \dots, Y_0(\mathbf{s}_{n'}^P))^\top$ at a set of n' unobserved locations $S_0^P = \{\mathbf{s}_1^P, \dots, \mathbf{s}_{n'}^P\}$.

We adopt the maximum likelihood method to estimate the unknown parameters Ω . The log-likelihood function is

$$\begin{aligned} l(\Omega) = & -\frac{n}{2} \log(2\pi) - \frac{1}{2} \log [\det \{C_0(S_0, S_0) + \tau^2 \mathbf{I}_n\}] \\ & - \frac{1}{2} \mathbf{Z}(S_0)^\top \{C_0(S_0, S_0) + \tau^2 \mathbf{I}_n\}^{-1} \mathbf{Z}(S_0), \end{aligned} \quad (1)$$

where $(C_0(S_0, S_0))_{ij} = C_0(\mathbf{s}_i, \mathbf{s}_j)$ ($i, j = 1, \dots, n$) and \mathbf{I}_n is an $n \times n$ identity matrix. After the parameter inference is completed, the spatial prediction is conducted by using the resulting maximum likelihood estimates. For the spatial prediction, we aim to obtain the predictive distribution

$$\begin{aligned} \mathbf{Y}_0(S_0^P) | \mathbf{Z}(S_0) \sim & \mathcal{N} \left(C_0(S_0^P, S_0) \{C_0(S_0, S_0) + \tau^2 \mathbf{I}_n\}^{-1} \mathbf{Z}(S_0), C_0(S_0^P, S_0^P) \right. \\ & \left. - C_0(S_0^P, S_0) \{C_0(S_0, S_0) + \tau^2 \mathbf{I}_n\}^{-1} C_0(S_0, S_0^P)^\top \right). \end{aligned} \quad (2)$$

(1) and (2) involve the determinant and/or inverse matrix of the $n \times n$ matrix $C_0(S_0, S_0) + \tau^2 \mathbf{I}_n$. The inverse matrix calculation requires $O(n^3)$ operations, which causes a formidable

computation when evaluating the log-likelihood function (1) and calculating both the mean vector and the covariance matrix in (2) for large spatial datasets. Furthermore, (1) and (2) require $O(n^2)$ memory, which often causes a lack of memory for large spatial datasets.

3 Multi-resolution approximation via linear projection

To address the computational burden, we propose the M -RA-lp. First, some notations are defined based on Katzfuss (2017) in order to describe the M -RA-lp concisely. Let m ($m = 0, \dots, M$) denote a resolution. For $m = 0, \dots, M$, D_{j_1, \dots, j_m} ($1 \leq j_i \leq J_i$, $2 \leq J_i$, $i = 1, \dots, M$) is obtained by partitioning the entire spatial domain D_0 and denotes a numbered subregion at the m th resolution. Throughout this paper, the index (j_1, \dots, j_m) and the index (j_1, \dots, j_m, a) for $m = 0$ correspond to the index 0 and the index a , respectively. For example, D_{j_1, \dots, j_m} for $m = 0$ is D_0 . The domain partitioning must satisfy the following assumption

$$D_{j_1, \dots, j_m} = \bigcup_{j_{m+1}=1, \dots, J_{m+1}} D_{j_1, \dots, j_m, j_{m+1}}, \quad D_{j_1, \dots, j_m, k} \cap D_{j_1, \dots, j_m, l} = \emptyset, \\ 1 \leq k \neq l \leq J_{m+1},$$

for $m = 0, \dots, M-1$. This assumption implies that each subregion is recursively divided into smaller disjoint subregions while increasing the resolution. We need to prespecify M and how to partition each D_{j_1, \dots, j_m} ($m = 0, \dots, M-1$). Let S_{j_1, \dots, j_m} be a subset of observed locations on D_{j_1, \dots, j_m} ($m = 0, \dots, M$).

Hereafter, for a generic notation X_{j_1, \dots, j_m} of a set, vector, or matrix, we assume that the stacked one of X_{j_1, \dots, j_m} is arranged in ascending order by the index (j_1, \dots, j_m) ($m = 1, \dots, M$). When comparing the number in order from the left of the index (j_1, \dots, j_m) , the first determined magnitude relationship is adopted as that of the index (j_1, \dots, j_m) . For example, if $|S_{j_1, \dots, j_m}| \geq 1$ where $|\cdot|$ denotes the size of the set, we can have the recursive expression $\mathbf{Z}(S_{j_1, \dots, j_m}) = (\mathbf{Z}(S_{j_1, \dots, j_m, 1})^\top, \mathbf{Z}(S_{j_1, \dots, j_m, 2})^\top, \dots, \mathbf{Z}(S_{j_1, \dots, j_m, J_{m+1}})^\top)^\top$ for $m = 0, \dots, M-1$.

We also need to select a set of knots on each subregion D_{j_1, \dots, j_m} which is denoted by Q_{j_1, \dots, j_m} ($m = 0, \dots, M$). Based on Katzfuss (2017), it is assumed that $Q_{j_1, \dots, j_m} = S_{j_1, \dots, j_m}$. The set of knots at the M th resolution is restrictive, but we can select Q_{j_1, \dots, j_m} , for example, as lattice points on D_{j_1, \dots, j_m} and a subset of S_{j_1, \dots, j_m} ($m = 0, \dots, M-1$). In simulation studies and the real data analysis of this paper, we select Q_{j_1, \dots, j_m} randomly from S_{j_1, \dots, j_m} .

($m = 0, \dots, M-1$). Moreover, we define $Q^{(m)} = \{Q_{j_1, \dots, j_m} | 1 \leq j_1 \leq J_1, \dots, 1 \leq j_m \leq J_m\}$ ($m = 0, \dots, M$).

Finally, we introduce an $r_{j_1, \dots, j_m} \times |Q_{j_1, \dots, j_m}|$ matrix Φ_{j_1, \dots, j_m} ($m = 0, \dots, M-1$, $1 \leq r_{j_1, \dots, j_m}$) where $\text{rank}(\Phi_{j_1, \dots, j_m}) = r_{j_1, \dots, j_m}$ and its row-norm is equal to 1. r_{j_1, \dots, j_m} is much smaller than the sample size n to avoid the computational burden. For $m = 0, \dots, M-1$, we define

$$\Phi^{(m)} = \begin{pmatrix} \Phi_{1, \dots, 1} & & O \\ & \ddots & \\ O & & \Phi_{J_1, \dots, J_m} \end{pmatrix}.$$

The selection of Φ_{j_1, \dots, j_m} will be discussed in Section 3.2.

Φ_{j_1, \dots, j_m} plays a critical role in the linear projection (see Banerjee et al., 2013; Hirano, 2017). In the linear projection, for $\mathbf{s} \in D_0$, we define

$$\begin{aligned} \tau_0(\mathbf{s}) &= E[Y_0(\mathbf{s}) | \Phi_0 \mathbf{Y}_0(Q_0)] \\ &= C_0(\mathbf{s}, Q_0) \Phi_0^\top \{ \Phi_0 C_0(Q_0, Q_0) \Phi_0^\top \}^{-1} \Phi_0 \mathbf{Y}_0(Q_0). \end{aligned}$$

Then, it follows that

$$\begin{aligned} C_{\tau_0}(\mathbf{s}_1, \mathbf{s}_2) &= \text{Cov}(\tau_0(\mathbf{s}_1), \tau_0(\mathbf{s}_2)) \\ &= C_0(\mathbf{s}_1, Q_0) \Phi_0^\top \hat{K}_0^0 \Phi_0 C_0(\mathbf{s}_2, Q_0)^\top, \end{aligned}$$

where $\hat{K}_0^0 = (\Phi_0 K_0^0 \Phi_0^\top)^{-1}$ and $K_0^0 = C_0(Q_0, Q_0)$. The linear projection uses C_{τ_0} as the main approximation of C_0 and is identical with the predictive process in the case of $\Phi_0 = \mathbf{I}_{|Q_0|}$. The simulation studies and real data analyses in Banerjee et al. (2013) demonstrated that it achieved better performance efficiently than that of the predictive process.

3.1 Algorithm for approximating the covariance function

In our proposed M -RA-lp, the calculation of C_{τ_0} is regarded as the linear projection at resolution 0, and the linear projection is applied repeatedly to its approximation error at resolutions $m = 1, \dots, M-1$. We will state the details of our proposed algorithm for approximating the covariance function.

Algorithm 1 (Approximation of the covariance function $C_0(\mathbf{s}_1^*, \mathbf{s}_2^*)$). Given $\mathbf{s}_1^*, \mathbf{s}_2^* \in D_0$, $M \geq 0$, D_{j_1, \dots, j_m} ($m = 1, \dots, M$, $1 \leq j_1 \leq J_1, \dots, 1 \leq j_m \leq J_m$), Q_{j_1, \dots, j_m} ($m = 0, \dots, M-1$, $1 \leq j_1 \leq J_1, \dots, 1 \leq j_{M-1} \leq J_{M-1}$), and $\gamma > 0$, find the approximated covariance function $C_{M\text{-RA-lp}}(\mathbf{s}_1^*, \mathbf{s}_2^*)$. If $M = 0$, output $C_{M\text{-RA-lp}}(\mathbf{s}_1^*, \mathbf{s}_2^*) = C_0(\mathbf{s}_1^*, \mathbf{s}_2^*)$. Otherwise, set $m = 0$ and $C_{M\text{-RA-lp}}(\mathbf{s}_1^*, \mathbf{s}_2^*) = 0$ initially.

Step 1. Set $C_{M\text{-RA-lp}}(\mathbf{s}_1^*, \mathbf{s}_2^*) = C_{M\text{-RA-lp}}(\mathbf{s}_1^*, \mathbf{s}_2^*) + C_{\tau_0}(\mathbf{s}_1^*, \mathbf{s}_2^*)$.

Step 2. When $m+1 < M$, if \mathbf{s}_1^* and \mathbf{s}_2^* are in the same subregion $D_{j_1^*, \dots, j_{m+1}^*}$, set $m = m+1$ and go to Step 3. When $m+1 = M$, if \mathbf{s}_1^* and \mathbf{s}_2^* are in the same subregion $D_{j_1^*, \dots, j_M^*}$, go to Step 4. Otherwise, go to Step 5.

Step 3. Define

$$C_m(\mathbf{s}_1, \mathbf{s}_2) = \begin{cases} C_{m-1}(\mathbf{s}_1, \mathbf{s}_2) - C_{\tau_{m-1}}(\mathbf{s}_1, \mathbf{s}_2), & \mathbf{s}_1, \mathbf{s}_2 \in D_{j_1, \dots, j_m} \\ & (1 \leq j_i \leq J_i, i = 1, \dots, m), \\ 0, & \text{otherwise.} \end{cases} \quad (3)$$

Next, for $\mathbf{s} \in D_0$, let $\delta_m(\mathbf{s}) \sim \text{GP}(0, C_m)$ be a zero-mean Gaussian process with the degenerate covariance function C_m . By conducting the linear projection for $\delta_m(\mathbf{s})$ at the m th resolution, we obtain

$$\begin{aligned} \tau_m(\mathbf{s}) &= E[\delta_m(\mathbf{s}) | \Phi^{(m)} \delta_m(Q^{(m)})] \\ &= C_m(\mathbf{s}, Q^{(m)}) \Phi^{(m)\top} \left\{ \Phi^{(m)} C_m(Q^{(m)}, Q^{(m)}) \Phi^{(m)\top} \right\}^{-1} \Phi^{(m)} \delta_m(Q^{(m)}) \end{aligned}$$

and

$$\begin{aligned} C_{\tau_m}(\mathbf{s}_1, \mathbf{s}_2) &= \text{Cov}(\tau_m(\mathbf{s}_1), \tau_m(\mathbf{s}_2)) \\ &= \begin{cases} C_m(\mathbf{s}_1, Q_{j_1, \dots, j_m}) \Phi_{j_1, \dots, j_m}^\top \hat{K}_{j_1, \dots, j_m}^m \Phi_{j_1, \dots, j_m} C_m(\mathbf{s}_2, Q_{j_1, \dots, j_m})^\top, \\ & \mathbf{s}_1, \mathbf{s}_2 \in D_{j_1, \dots, j_m} \quad (1 \leq j_i \leq J_i, i = 1, \dots, m), \\ 0, & \text{otherwise,} \end{cases} \end{aligned} \quad (4)$$

where $\hat{K}_{j_1, \dots, j_m}^m = (\Phi_{j_1, \dots, j_m} K_{j_1, \dots, j_m}^m \Phi_{j_1, \dots, j_m}^\top)^{-1}$ and $K_{j_1, \dots, j_m}^m = C_m(Q_{j_1, \dots, j_m}, Q_{j_1, \dots, j_m})$. Set $C_{M\text{-RA-lp}}(\mathbf{s}_1^*, \mathbf{s}_2^*) = C_{M\text{-RA-lp}}(\mathbf{s}_1^*, \mathbf{s}_2^*) + C_{\tau_m}(\mathbf{s}_1^*, \mathbf{s}_2^*)$ and go to Step 2.

Step 4. Define

$$C_M(\mathbf{s}_1, \mathbf{s}_2) = \begin{cases} C_{M-1}(\mathbf{s}_1, \mathbf{s}_2) - C_{\tau_{M-1}}(\mathbf{s}_1, \mathbf{s}_2), & \mathbf{s}_1, \mathbf{s}_2 \in D_{j_1, \dots, j_M} \\ & (1 \leq j_i \leq J_i, i = 1, \dots, M), \\ 0, & \text{otherwise.} \end{cases} \quad (5)$$

Set $C_{M\text{-RA-lp}}(\mathbf{s}_1^*, \mathbf{s}_2^*) = C_{M\text{-RA-lp}}(\mathbf{s}_1^*, \mathbf{s}_2^*) + C_M(\mathbf{s}_1^*, \mathbf{s}_2^*) T_\gamma(\mathbf{s}_1^*, \mathbf{s}_2^*)$ where $T_\gamma(\mathbf{s}_1, \mathbf{s}_2)$ ($\gamma > 0$, $\mathbf{s}_1, \mathbf{s}_2 \in D_0$) is a compactly supported correlation function with $T_\gamma(\mathbf{s}_1, \mathbf{s}_2) = 0$ for $\|\mathbf{s}_1 - \mathbf{s}_2\| \geq \gamma$, and $\|\cdot\|$ denotes the Euclidean norm.

Step 5. Output $C_{M\text{-RA-lp}}(\mathbf{s}_1^*, \mathbf{s}_2^*)$.

Step 3 represents the linear projection at the m th resolution. In order to derive the fast computation algorithms in Section 4, $C_m(\mathbf{s}_1, \mathbf{s}_2)$ is defined as 0 if \mathbf{s}_1 and \mathbf{s}_2 do not belong to the same subregion at the m th resolution for $m = 1, \dots, M$. For the same reason, we introduce T_γ in Step 4. Some compactly supported correlation functions have been

developed (see, e.g., Wendland, 1995; Gneiting, 2002; Bevilacqua et al., 2019). Examples of these types of functions include the spherical covariance function

$$T_\gamma(\mathbf{s}_1, \mathbf{s}_2) = \left(1 - \frac{\|\mathbf{s}_1 - \mathbf{s}_2\|}{\gamma}\right)_+^2 \left(1 + \frac{\|\mathbf{s}_1 - \mathbf{s}_2\|}{2\gamma}\right)$$

and the Wendland₂ taper function (see Wendland, 1995; Furrer et al., 2006):

$$T_\gamma(\mathbf{s}_1, \mathbf{s}_2) = \left(1 - \frac{\|\mathbf{s}_1 - \mathbf{s}_2\|}{\gamma}\right)_+^6 \left(1 + \frac{6\|\mathbf{s}_1 - \mathbf{s}_2\|}{\gamma} + \frac{35\|\mathbf{s}_1 - \mathbf{s}_2\|^2}{3\gamma^2}\right).$$

For simplicity, we use the spherical covariance function as T_γ in this paper.

If $|S_{j_1, \dots, j_M}| \geq 1$, the covariance matrix by using $C_{M\text{-RA-lp}}$ defined by Algorithm 1 is

$$\begin{aligned} C_{M\text{-RA-lp}}(S_0, S_0) &= \sum_{m=0}^{M-1} C_{\tau_m}(S_0, S_0) + C_M(S_0, S_0) \circ T_\gamma(S_0, S_0) \\ &= B_0^0 \Phi_0^\top \hat{K}_0^0 \Phi_0 B_0^{0\top} \\ &\quad + \begin{pmatrix} B_1^1 & & O \\ & \ddots & \\ O & & B_{J_1}^1 \end{pmatrix} \begin{pmatrix} \Phi_1^\top & & O \\ & \ddots & \\ O & & \Phi_{J_1}^\top \end{pmatrix} \begin{pmatrix} \hat{K}_1^1 & & O \\ & \ddots & \\ O & & \hat{K}_{J_1}^1 \end{pmatrix} \begin{pmatrix} \Phi_1 & & O \\ & \ddots & \\ O & & \Phi_{J_1} \end{pmatrix} \\ &\quad \times \begin{pmatrix} B_1^{1\top} & & O \\ & \ddots & \\ O & & B_{J_1}^{1\top} \end{pmatrix} \\ &\quad \vdots \\ &\quad + \begin{pmatrix} B_{1, \dots, 1}^{M-1} & & O \\ & \ddots & \\ O & & B_{J_1, \dots, J_{M-1}}^{M-1} \end{pmatrix} \begin{pmatrix} \Phi_{1, \dots, 1}^\top & & O \\ & \ddots & \\ O & & \Phi_{J_1, \dots, J_{M-1}}^\top \end{pmatrix} \begin{pmatrix} \hat{K}_{1, \dots, 1}^{M-1} & & O \\ & \ddots & \\ O & & \hat{K}_{J_1, \dots, J_{M-1}}^{M-1} \end{pmatrix} \\ &\quad \times \begin{pmatrix} \Phi_{1, \dots, 1} & & O \\ & \ddots & \\ O & & \Phi_{J_1, \dots, J_{M-1}} \end{pmatrix} \begin{pmatrix} B_{1, \dots, 1}^{M-1\top} & & O \\ & \ddots & \\ O & & B_{J_1, \dots, J_{M-1}}^{M-1\top} \end{pmatrix} \\ &\quad + \begin{pmatrix} C_M(S_{1, \dots, 1}, S_{1, \dots, 1}) & & O \\ & \ddots & \\ O & & C_M(S_{J_1, \dots, J_M}, S_{J_1, \dots, J_M}) \end{pmatrix} \circ T_\gamma(S_0, S_0), \end{aligned} \quad (6)$$

where $B_{j_1, \dots, j_m}^m = C_m(S_{j_1, \dots, j_m}, Q_{j_1, \dots, j_m})$ ($m = 0, \dots, M-1$), and the symbol “ \circ ” refers to the Hadamard product. For $m = 0, \dots, M-1$, the $(m+1)$ st term in (6) corresponds to the linear projection at the m th resolution. We observed that the linear projection at the higher resolution improved the approximation of the original covariance function on smaller and smaller scales. Consequently, the overlap between the covariance tapering at the highest resolution and the effect of iterative approximation in the M -RA-lp can occur. By selecting low M , we may be able to bypass the redundant overlap. Moreover,

for large M , the approximated covariance functions up to resolution m ($m = 0, \dots, M$) in Algorithm 1, that is, the summation up to the $(m + 1)$ st term in (6), are often almost unchanged at high resolutions. This fact provides us with suggestions on selecting an appropriate M .

The following proposition proves the theoretical properties associated with Algorithm 1. Note that the case of $M = 0$ in the following proposition is excluded because the validity of Algorithm 1 is clear from $C_{M\text{-RA-lp}} = C_0$ when $M = 0$.

Proposition 1. Given $M \geq 1$, D_{j_1, \dots, j_m} ($m = 1, \dots, M$, $1 \leq j_1 \leq J_1, \dots, 1 \leq j_M \leq J_M$), Q_{j_1, \dots, j_m} ($m = 0, \dots, M - 1$, $1 \leq j_1 \leq J_1, \dots, 1 \leq j_{M-1} \leq J_{M-1}$), and $\gamma > 0$, suppose that Φ_{j_1, \dots, j_m} , which satisfies $R(\Phi_{j_1, \dots, j_m}^\top) \cap R(K_{j_1, \dots, j_m}^m)^\perp = \{\mathbf{0}\}$ ($m = 1, \dots, M - 1$) if $M \geq 2$, is selected where $R(\cdot)$ means the column space of \cdot , the symbol “ \perp ” refers to the orthogonal complement, and $\mathbf{0}$ is the zero vector.

- (a) For $m = 1, \dots, M$, C_m is a positive semidefinite function.
- (b) For $m = 0, \dots, M - 1$, $\Phi_{j_1, \dots, j_m} K_{j_1, \dots, j_m}^m \Phi_{j_1, \dots, j_m}^\top$ is positive definite.
- (c) $C_{M\text{-RA-lp}}$ is a positive semidefinite function.
- (d) If $\mathbf{s}_1 = \mathbf{s}_2$, then $C_{M\text{-RA-lp}}(\mathbf{s}_1, \mathbf{s}_2) = C_0(\mathbf{s}_1, \mathbf{s}_2)$.

For example, if the normalized vectors selected from $R(K_{j_1, \dots, j_m}^m)$ can be used as the linearly independent column vectors of $\Phi_{j_1, \dots, j_m}^\top$ in Step 3 of Algorithm 1, the assumption of Proposition 1 is satisfied. For $m = 1, \dots, M - 1$, if $K_{j_1, \dots, j_m}^m = O$, this assumption does not hold because of the definition of Φ_{j_1, \dots, j_m} . Proposition 1 (b) guarantees the existence of inverse matrices in Step 3 of Algorithm 1. In Section 4, we propose the two fast computation algorithms of the log-likelihood function and predictive distribution defined by replacing C_0 in (1) and (2) with $C_{M\text{-RA-lp}}$. Proposition 1 (c) guarantees the existence of the inverse matrix of $C_{M\text{-RA-lp}}(S_0, S_0) + \tau^2 \mathbf{I}_n$ appearing in this replacement. Propositions 1 (a) and (c) are the linear projection versions of the results in the proof of Proposition 1 of Katzfuss (2017). Proposition 1 (d) states that Algorithm 1 completely recovers the variance of the original Gaussian process.

3.2 Selection of Φ_{j_1, \dots, j_m}

We will discuss how to select Φ_{j_1, \dots, j_m} in the linear projection at each resolution based on the argument of Section 3.1 of Banerjee et al. (2013). Now, we consider the case of $\Phi_{j_1, \dots, j_m}^\top = U_{j_1, \dots, j_m}^{(r_{j_1, \dots, j_m})}$ where $U_{j_1, \dots, j_m}^{(r_{j_1, \dots, j_m})}$ is a $|Q_{j_1, \dots, j_m}| \times r_{j_1, \dots, j_m}$ matrix whose i th column vector is the eigenvector corresponding to the i th eigenvalue of the positive semidefinite matrix K_{j_1, \dots, j_m}^m in descending order of magnitude ($i = 1, \dots, r_{j_1, \dots, j_m}$). Suppose that $r_{j_1, \dots, j_m} < \text{rank}(K_{j_1, \dots, j_m}^m)$ is satisfied. Since $R(\Phi_{j_1, \dots, j_m}^\top) = R(U_{j_1, \dots, j_m}^{(r_{j_1, \dots, j_m})}) \subset R(K_{j_1, \dots, j_m}^m)$

and $R(K_{j_1, \dots, j_m}^m) \cap R(K_{j_1, \dots, j_m}^m)^\perp = \{\mathbf{0}\}$, it follows that $R(\Phi_{j_1, \dots, j_m}^\top) \cap R(K_{j_1, \dots, j_m}^m)^\perp = \{\mathbf{0}\}$. In addition, from Schmidt's approximation theorem (see Stewart, 1993; Puntanen et al., 2011), $C_{\tau_m}(Q_{j_1, \dots, j_m}, Q_{j_1, \dots, j_m}) = K_{j_1, \dots, j_m}^m \Phi_{j_1, \dots, j_m}^\top \hat{K}_{j_1, \dots, j_m}^m \Phi_{j_1, \dots, j_m} K_{j_1, \dots, j_m}^m$ is the best rank- r_{j_1, \dots, j_m} approximation of $C_m(Q_{j_1, \dots, j_m}, Q_{j_1, \dots, j_m}) = K_{j_1, \dots, j_m}^m$ in the sense of the Frobenius norm for matrices. Therefore, one reasonable selection is $\Phi_{j_1, \dots, j_m}^\top = U_{j_1, \dots, j_m}^{(r_{j_1, \dots, j_m})}$, but the derivation of eigenvalues and eigenvectors of K_{j_1, \dots, j_m}^m involves $O(|Q_{j_1, \dots, j_m}|^3)$ computations (Golub and Van Loan, 2012).

To address this problem, Banerjee et al. (2013) used a stochastic matrix approximation technique to find Φ_0 in the linear projection at resolution 0 on the basis of Algorithm 4.2 of Halko et al. (2011). Banerjee et al. (2013) and Hirano (2017) demonstrated its effectiveness in practice through simulation studies and real data analyses. Thus, in this paper, we implement this technique at each resolution, which enables us to obtain Φ_{j_1, \dots, j_m} efficiently. However, whether the selected Φ_{j_1, \dots, j_m} satisfies the assumption of Proposition 1 rigorously is a future study.

The following algorithm corresponds to Algorithm 2 of Banerjee et al. (2013) at each resolution.

Algorithm 2 (Selection of Φ_{j_1, \dots, j_m} (Halko et al., 2011; Banerjee et al., 2013)). Given K_{j_1, \dots, j_m}^m , a target error $\varepsilon > 0$, and $c \in \mathbb{N}^+$, find the $r_{j_1, \dots, j_m} \times |Q_{j_1, \dots, j_m}|$ matrix Φ_{j_1, \dots, j_m} for $m = 0, \dots, M-1$. The selected Φ_{j_1, \dots, j_m} satisfies $\|K_{j_1, \dots, j_m}^m - \Phi_{j_1, \dots, j_m}^\top \Phi_{j_1, \dots, j_m} K_{j_1, \dots, j_m}^m\|_F < \varepsilon$ with probability $1 - |Q_{j_1, \dots, j_m}|/10^c$ where $\|\cdot\|_F$ denotes the Frobenius norm for matrices.

Step 1. Initially, set $j = 0$ and $\Phi_{j_1, \dots, j_m}^{(0)} = []$, which is the $0 \times |Q_{j_1, \dots, j_m}|$ empty matrix.

Step 2. Draw c length- $|Q_{j_1, \dots, j_m}|$ random vectors $\boldsymbol{\omega}^{(1)}, \dots, \boldsymbol{\omega}^{(c)}$ with independent entries from $\mathcal{N}(0, 1)$.

Step 3. Calculate $\boldsymbol{\kappa}^{(i)} = K_{j_1, \dots, j_m}^m \boldsymbol{\omega}^{(i)}$ for $i = 1, \dots, c$.

Step 4. Check whether $\max_{i=1, \dots, c} (\|\boldsymbol{\kappa}^{(i+j)}\|) < \{(\pi/2)^{1/2} \varepsilon\}/10$. If it holds, go to Step 11. Otherwise, go to Step 5.

Step 5. Set $j = j + 1$. Recalculate $\boldsymbol{\kappa}^{(j)} = \left(\mathbf{I}_{|Q_{j_1, \dots, j_m}|} - \Phi_{j_1, \dots, j_m}^{(j-1)\top} \Phi_{j_1, \dots, j_m}^{(j-1)} \right) \boldsymbol{\kappa}^{(j)}$ and $\boldsymbol{\phi}^{(j)} = \boldsymbol{\kappa}^{(j)} / \|\boldsymbol{\kappa}^{(j)}\|$.

Step 6. Set $\Phi_{j_1, \dots, j_m}^{(j)} = \left[\Phi_{j_1, \dots, j_m}^{(j-1)\top} \quad \boldsymbol{\phi}^{(j)} \right]^\top$, which stands for the concatenation of the matrix and row vector.

Step 7. Draw a length- $|Q_{j_1, \dots, j_m}|$ random vector $\boldsymbol{\omega}^{(j+c)}$ with independent entries from $\mathcal{N}(0, 1)$.

Step 8. Calculate $\boldsymbol{\kappa}^{(j+c)} = \left(\mathbf{I}_{|Q_{j_1, \dots, j_m}|} - \Phi_{j_1, \dots, j_m}^{(j)\top} \Phi_{j_1, \dots, j_m}^{(j)} \right) K_{j_1, \dots, j_m}^m \boldsymbol{\omega}^{(j+c)}$.

Step 9. Recalculate $\boldsymbol{\kappa}^{(i)} = \boldsymbol{\kappa}^{(i)} - \boldsymbol{\phi}^{(j)} \left(\boldsymbol{\phi}^{(j)\top} \boldsymbol{\kappa}^{(i)} \right)$ for $i = j + 1, \dots, j + c - 1$.

Step 10. Go back to the target error check in Step 4.

Step 11. If $j = 0$, output $\Phi_{j_1, \dots, j_m} = (\kappa^{(1)} / \|\kappa^{(1)}\|)^\top$. Otherwise, output $\Phi_{j_1, \dots, j_m} = \Phi_{j_1, \dots, j_m}^{(j)}$.

From $U_{j_1, \dots, j_m}^{(r_{j_1, \dots, j_m})} U_{j_1, \dots, j_m}^{(r_{j_1, \dots, j_m})^\top} K_{j_1, \dots, j_m}^m = K_{j_1, \dots, j_m}^m U_{j_1, \dots, j_m}^{(r_{j_1, \dots, j_m})} \left(U_{j_1, \dots, j_m}^{(r_{j_1, \dots, j_m})^\top} K_{j_1, \dots, j_m}^m U_{j_1, \dots, j_m}^{(r_{j_1, \dots, j_m})} \right)^{-1} \times U_{j_1, \dots, j_m}^{(r_{j_1, \dots, j_m})^\top} K_{j_1, \dots, j_m}^m$, Algorithm 2 aims to select the appropriate Φ_{j_1, \dots, j_m} by diminishing $\|K_{j_1, \dots, j_m}^m - \Phi_{j_1, \dots, j_m}^\top \Phi_{j_1, \dots, j_m} K_{j_1, \dots, j_m}^m\|_F$ for any target error level. The projection of Step 5 is introduced in order to ensure better numerical stability (see Halko et al., 2011). In our implementation of Algorithm 2, we used c such that $|Q_{j_1, \dots, j_m}| / 10^c \approx 0.1$.

4 Inference

In this section, we propose the two algorithms to conduct fast computation of (1) and (2) where C_0 is replaced with $C_{M\text{-RA-lp}}$ defined by Algorithm 1. Consequently, just by using the subsequent two algorithms, we can conduct the likelihood-based inference on the parameters Ω and obtain the spatial predictive distribution. In what follows, it is assumed that $|S_{j_1, \dots, j_M}| \geq 1$ for simplicity.

4.1 Parameter estimation

The log-likelihood function replaced by the approximated covariance function $C_{M\text{-RA-lp}}$ instead of C_0 is given by

$$-\frac{n}{2} \log(2\pi) - \frac{1}{2} \log [\det \{C_{M\text{-RA-lp}}(S_0, S_0) + \tau^2 \mathbf{I}_n\}] - \frac{1}{2} \mathbf{Z}(S_0)^\top \{C_{M\text{-RA-lp}}(S_0, S_0) + \tau^2 \mathbf{I}_n\}^{-1} \mathbf{Z}(S_0). \quad (7)$$

We will elicit the algorithm to calculate (7) efficiently in accordance with the arguments in Sections 3.1–3.3 of Katzfuss (2017). For $m = 0, \dots, M-1$, we define

$$\Sigma_{j_1, \dots, j_m} = B_{j_1, \dots, j_m}^m \Phi_{j_1, \dots, j_m}^\top \hat{K}_{j_1, \dots, j_m}^m \Phi_{j_1, \dots, j_m} B_{j_1, \dots, j_m}^{m^\top} + V_{j_1, \dots, j_m}, \quad (8)$$

$$V_{j_1, \dots, j_m} = \begin{pmatrix} \Sigma_{j_1, \dots, j_m, 1} & & O \\ & \ddots & \\ O & & \Sigma_{j_1, \dots, j_m, J_{m+1}} \end{pmatrix}, \quad (9)$$

where $\Sigma_{j_1, \dots, j_m} = K_{j_1, \dots, j_m}^M \circ T_\gamma(S_{j_1, \dots, j_m}, S_{j_1, \dots, j_m}) + \tau^2 \mathbf{I}_{|S_{j_1, \dots, j_m}|}$ and $K_{j_1, \dots, j_m}^M = C_M(S_{j_1, \dots, j_m}, S_{j_1, \dots, j_m}) = C_M(Q_{j_1, \dots, j_m}, Q_{j_1, \dots, j_m})$ because $Q_{j_1, \dots, j_m} = S_{j_1, \dots, j_m}$. From (6), (8), and (9), it follows that $\Sigma_0 = C_{M\text{-RA-lp}}(S_0, S_0) + \tau^2 \mathbf{I}_n$. Moreover, we introduce some comprehensive definitions $K_{j_1, \dots, j_m}^k = C_k(Q_{j_1, \dots, j_k}, Q_{j_1, \dots, j_m})$ ($0 \leq k \leq m$, $m = 0, \dots, M$) and $B_{j_1, \dots, j_m}^k = C_k(S_{j_1, \dots, j_m}, Q_{j_1, \dots, j_k})$ ($0 \leq k \leq m$, $m = 0, \dots, M$).

Next, we describe the algorithm to calculate efficiently the approximated log-likelihood function (7) (see Appendix C.2 for the derivation of the algorithm).

Algorithm 3 (Efficient computation of the approximated log-likelihood function (7)).

Given $M > 0$, D_{j_1, \dots, j_m} ($m = 1, \dots, M$, $1 \leq j_1 \leq J_1, \dots, 1 \leq j_m \leq J_m$), Q_{j_1, \dots, j_m} ($m = 0, \dots, M-1$, $1 \leq j_1 \leq J_1, \dots, 1 \leq j_{M-1} \leq J_{M-1}$), and $\gamma > 0$, find $d_0 = \log [\det \{C_{M\text{-RA-lp}}(S_0, S_0) + \tau^2 \mathbf{I}_n\}]$ and $u_0 = \mathbf{Z}(S_0)^\top \{C_{M\text{-RA-lp}}(S_0, S_0) + \tau^2 \mathbf{I}_n\}^{-1} \mathbf{Z}(S_0)$.

Step 1. For $0 \leq k \leq m$, $m = 0, \dots, M$, it follows that

$$K_{j_1, \dots, j_m}^k = \begin{cases} C_0(Q_0, Q_{j_1, \dots, j_m}), & k = 0, \\ C_0(Q_{j_1, \dots, j_k}, Q_{j_1, \dots, j_m}) \\ - \sum_{l=0}^{k-1} K_{j_1, \dots, j_k}^{l\top} \Phi_{j_1, \dots, j_l}^\top \hat{K}_{j_1, \dots, j_l}^l \Phi_{j_1, \dots, j_l} K_{j_1, \dots, j_m}^l, & 1 \leq k \leq m. \end{cases} \quad (10)$$

Calculate K_{j_1, \dots, j_m}^m ($m = 0, \dots, M$), $B_{j_1, \dots, j_M}^k = K_{j_1, \dots, j_M}^{k\top}$ ($k = 0, \dots, M-1$), and Φ_{j_1, \dots, j_m} ($m = 0, \dots, M-1$) by starting with K_{j_1, \dots, j_m}^0 ($m = 0, \dots, M$) as the initial matrix. Φ_{j_1, \dots, j_m} is obtained by applying Algorithm 2 to K_{j_1, \dots, j_m}^m .

Step 2. Calculate $\tilde{A}_{j_1, \dots, j_M}^{k,l} = B_{j_1, \dots, j_M}^{k\top} \Sigma_{j_1, \dots, j_M}^{-1} B_{j_1, \dots, j_M}^l$ ($0 \leq k \leq l < M$).

Step 3. For $0 \leq k \leq l \leq m$, $m = 0, \dots, M-1$, we have

$$A_{j_1, \dots, j_m}^{k,l} = \sum_{j_{m+1}=1}^{J_{m+1}} \tilde{A}_{j_1, \dots, j_m, j_{m+1}}^{k,l}. \quad (11)$$

Now, we define $\tilde{K}_{j_1, \dots, j_m}^m = \left(\hat{K}_{j_1, \dots, j_m}^{m-1} + \Phi_{j_1, \dots, j_m} A_{j_1, \dots, j_m}^{m,m} \Phi_{j_1, \dots, j_m}^\top \right)^{-1}$ for $m = 0, \dots, M-1$.

For $0 \leq k \leq l < m$, $m = 1, \dots, M-1$, it follows that

$$\tilde{A}_{j_1, \dots, j_m}^{k,l} = A_{j_1, \dots, j_m}^{k,l} - A_{j_1, \dots, j_m}^{k,m} \Phi_{j_1, \dots, j_m}^\top \tilde{K}_{j_1, \dots, j_m}^m \Phi_{j_1, \dots, j_m} A_{j_1, \dots, j_m}^{m,l}, \quad (12)$$

where $A_{j_1, \dots, j_m}^{m,l} = A_{j_1, \dots, j_m}^{l,m\top}$. Calculate $A_{j_1, \dots, j_m}^{k,l}$ ($0 \leq k \leq l \leq m$, $m = M-1, \dots, 0$) by using (11) and (12) alternately from $\tilde{A}_{j_1, \dots, j_M}^{k,l}$ of Step 2 as the initial matrix.

Step 4. Calculate $\tilde{\omega}_{j_1, \dots, j_M}^k = B_{j_1, \dots, j_M}^{k\top} \Sigma_{j_1, \dots, j_M}^{-1} \mathbf{Z}(S_{j_1, \dots, j_M})$ ($0 \leq k < M$).

Step 5. For $0 \leq k \leq m$, $m = 0, \dots, M-1$, we have

$$\omega_{j_1, \dots, j_m}^k = \sum_{j_{m+1}=1}^{J_{m+1}} \tilde{\omega}_{j_1, \dots, j_m, j_{m+1}}^k. \quad (13)$$

For $0 \leq k < m$, $m = 1, \dots, M-1$, it follows that

$$\tilde{\omega}_{j_1, \dots, j_m}^k = \omega_{j_1, \dots, j_m}^k - A_{j_1, \dots, j_m}^{k,m} \Phi_{j_1, \dots, j_m}^\top \tilde{K}_{j_1, \dots, j_m}^m \Phi_{j_1, \dots, j_m} \omega_{j_1, \dots, j_m}^m. \quad (14)$$

Calculate $\omega_{j_1, \dots, j_m}^m$ ($m = M-1, \dots, 0$) by using (13) and (14) alternately from $\tilde{\omega}_{j_1, \dots, j_M}^k$ of Step 4 as the initial vector.

Step 6. Calculate $d_{j_1, \dots, j_M} = \log \{\det (\Sigma_{j_1, \dots, j_M})\}$ and $u_{j_1, \dots, j_M} = \mathbf{Z}(S_{j_1, \dots, j_M})^\top \Sigma_{j_1, \dots, j_M}^{-1} \mathbf{Z}(S_{j_1, \dots, j_M})$.

Step 7. For $m = 0, \dots, M-1$, it follows that

$$d_{j_1, \dots, j_m} = -\log \left\{ \det \left(\tilde{K}_{j_1, \dots, j_m}^m \right) \right\} + \log \left\{ \det \left(\hat{K}_{j_1, \dots, j_m}^m \right) \right\} + \sum_{j_{m+1}=1}^{J_{m+1}} d_{j_1, \dots, j_m, j_{m+1}}, \quad (15)$$

$$u_{j_1, \dots, j_m} = -\omega_{j_1, \dots, j_m}^{m^\top} \Phi_{j_1, \dots, j_m}^\top \tilde{K}_{j_1, \dots, j_m}^m \Phi_{j_1, \dots, j_m} \omega_{j_1, \dots, j_m}^m + \sum_{j_{m+1}=1}^{J_{m+1}} u_{j_1, \dots, j_m, j_{m+1}}. \quad (16)$$

Calculate d_0 and u_0 by using (15) and (16) recursively from d_{j_1, \dots, j_M} and u_{j_1, \dots, j_M} of Step 6 as the initial values, respectively.

Step 8. Output d_0 and u_0 .

Indeed, (7) is evaluated by using only Algorithm 3 without Algorithm 1. In Steps 1–6 of Algorithm 3, we calculate the matrices required to obtain d_0 and u_0 from d_{j_1, \dots, j_M} and u_{j_1, \dots, j_M} . Note that if $M = 1$, then (12) and (14) are not calculated. Also, all of $A_{j_1, \dots, j_m}^{k, l}$ ($0 \leq k \leq l \leq m$, $m = M-1, \dots, 0$) calculated in Step 3 are not necessarily used in the subsequent steps.

Algorithm 3 does not include the inverse of an $n \times n$ matrix. There are the inverse and determinant of the $|S_{j_1, \dots, j_M}| \times |S_{j_1, \dots, j_M}|$ sparse matrices Σ_{j_1, \dots, j_M} and $r_{j_1, \dots, j_m} \times r_{j_1, \dots, j_m}$ matrices ($r_{j_1, \dots, j_m} \ll n$), and we can calculate them efficiently.

In order to discuss the operation count and storage of Algorithm 3, we assume for simplicity that $J_i = J$, $|Q_{j_1, \dots, j_m}| = r$ ($m = 0, \dots, M-1$), $r_{j_1, \dots, j_m} = O(r)$ ($m = 0, \dots, M-1$), and $|S_{j_1, \dots, j_M}| = n/(J^M) > r$ only in the discussion on the time and memory complexity. When J , M , and r are large, the main computational efforts are the calculations of $\tilde{A}_{j_1, \dots, j_m}^{k, l}$ ($0 \leq k \leq l < m$, $1 \leq j_m \leq J$, $m = 1, \dots, M-1$) and K_{j_1, \dots, j_m}^k ($0 \leq k \leq m$, $m = 0, \dots, M-1$, $1 \leq j_i \leq J$, $i = 1, \dots, M-1$). From $\sum_{m=0}^{M-1} J^m < J^M$, they are $O(J^M M^2 r^3)$ for the operation count. Similarly, the computational burden of Algorithm 2 also increases because we need to implement Algorithm 2 $O(J^M)$ times. Algorithm 2 uses the $r \times r$ matrix K_{j_1, \dots, j_m}^m ($m = 0, \dots, M-1$) as the input matrix, and its operation count does not depend on n . The fourth simulation of Section 5.1 indicates that we can rapidly implement Algorithm 2 $O(J^M)$ times by selecting small r and r_{j_1, \dots, j_m} even for large J and M . When n is large, the computational bottleneck of Algorithm 3 is in obtaining K_{j_1, \dots, j_M}^k ($0 \leq k \leq M$, $1 \leq j_i \leq J$, $i = 1, \dots, M$) which is $O(n^3 M^2 / (J^{2M}))$ for the operation count. This means that large J and M make the computation of the matrices K_{j_1, \dots, j_M}^k fast. In addition, calculations related to the inverse of the sparse matrix Σ_{j_1, \dots, j_M} could also be the computational bottleneck if the sparsity of Σ_{j_1, \dots, j_M} is insufficient. It is difficult to evaluate the exact computational cost of the Cholesky decomposition of the sparse matrix because it depends on the number of non-zero elements and on the ordering of locations. However, its resulting time complexity can be less than $O(n^3)$.

(see Section 3.3 of Furrer et al., 2006, for details). Large J and M lead to the small size of Σ_{j_1, \dots, j_M} and J^M Cholesky decompositions of the sparse matrix Σ_{j_1, \dots, j_M} . Through some simulations, we observed that large J and M usually reduced the total computation time related to the inverse of sparse matrix. The unignorable bottlenecks of the memory consumption of Algorithm 3 are B_{j_1, \dots, j_M}^k ($0 \leq k \leq M-1$, $1 \leq j_i \leq J$, $i = 1, \dots, M$) and K_{j_1, \dots, j_M}^M ($1 \leq j_i \leq J$, $i = 1, \dots, M$) which are $O(nMr)$ and $O(n^2/(J^M))$ for the storage, respectively. Furthermore, the memory complexities including J^M as the product do not depend on n . Also, the memory consumption in Algorithm 2 is independent of n , and the sparse matrix Σ_{j_1, \dots, j_M} requires at most $O(n^2/(J^{2M}))$ memory. Thus, Algorithm 3 can avoid $O(n^3)$ operations and $O(n^2)$ memory.

Finally, Algorithm 3 can be parallelized except for Step 1. We introduce a parallel version of Algorithm 3 (see Algorithm 5 in Appendix D.1).

4.2 Spatial prediction

Similar to Section 4.1, we will propose the algorithm for fast computation of the predictive distribution replaced by the approximated covariance function $C_{M\text{-RA-lp}}$ instead of C_0 . Let S_{j_1, \dots, j_M}^P denote the set of the unobserved locations on D_{j_1, \dots, j_M} . Additionally, we define $B_{j_1, \dots, j_M}^{l,P} = C_l(S_{j_1, \dots, j_M}^P, Q_{j_1, \dots, j_l})$ ($0 \leq l \leq M$). The approximated predictive distribution for $\mathbf{Y}_0(S_{j_1, \dots, j_M}^P)$ given $\mathbf{Z}(S_0)$ is the normal distribution with the mean vector

$$C_{M\text{-RA-lp}}(S_{j_1, \dots, j_M}^P, S_0) \{C_{M\text{-RA-lp}}(S_0, S_0) + \tau^2 \mathbf{I}_n\}^{-1} \mathbf{Z}(S_0) \quad (17)$$

and covariance matrix

$$\begin{aligned} & C_{M\text{-RA-lp}}(S_{j_1, \dots, j_M}^P, S_{j_1, \dots, j_M}^P) - C_{M\text{-RA-lp}}(S_{j_1, \dots, j_M}^P, S_0) \\ & \times \{C_{M\text{-RA-lp}}(S_0, S_0) + \tau^2 \mathbf{I}_n\}^{-1} C_{M\text{-RA-lp}}(S_{j_1, \dots, j_M}^P, S_0)^\top. \end{aligned} \quad (18)$$

The following algorithm allows us to calculate efficiently (17) and (18) (see Appendix C.3 for the derivation of the algorithm). Note that the index (j_1, \dots, j_M) of S_{j_1, \dots, j_M}^P is fixed.

Algorithm 4 (Efficient computation of (17) and (18)). Given $M > 0$, $D_{j'_1, \dots, j'_m}$ ($m = 1, \dots, M$, $1 \leq j'_1 \leq J_1, \dots, 1 \leq j'_M \leq J_M$), $Q_{j'_1, \dots, j'_m}$ ($m = 0, \dots, M-1$, $1 \leq j'_1 \leq J_1, \dots, 1 \leq j'_{M-1} \leq J_{M-1}$), $\gamma > 0$, and S_{j_1, \dots, j_M}^P , find $\boldsymbol{\mu}_{j_1, \dots, j_M}^0 = C_{M\text{-RA-lp}}(S_{j_1, \dots, j_M}^P, S_0) \times \{C_{M\text{-RA-lp}}(S_0, S_0) + \tau^2 \mathbf{I}_n\}^{-1} \mathbf{Z}(S_0)$ and $\Psi_{j_1, \dots, j_M}^0 = C_{M\text{-RA-lp}}(S_{j_1, \dots, j_M}^P, S_{j_1, \dots, j_M}^P) - C_{M\text{-RA-lp}}(S_{j_1, \dots, j_M}^P, S_0) \{C_{M\text{-RA-lp}}(S_0, S_0) + \tau^2 \mathbf{I}_n\}^{-1} C_{M\text{-RA-lp}}(S_{j_1, \dots, j_M}^P, S_0)^\top$.

Step 1. Conduct Steps 1–3 in Algorithm 3. Moreover, if $M \geq 2$, calculate also K_{j_1, \dots, j_l}^k ($0 \leq k \leq l-1$, $1 \leq l \leq M-1$) for the fixed (j_1, \dots, j_M) .

Step 2. For $0 \leq l \leq M$, it follows that

$$B_{j_1, \dots, j_M}^{l,P} = \begin{cases} C_0(S_{j_1, \dots, j_M}^P, Q_0), & l = 0, \\ C_0(S_{j_1, \dots, j_M}^P, Q_{j_1, \dots, j_l}) \\ - \sum_{k=0}^{l-1} B_{j_1, \dots, j_M}^{k,P} \Phi_{j_1, \dots, j_k}^\top \widehat{K}_{j_1, \dots, j_k}^k \Phi_{j_1, \dots, j_k} K_{j_1, \dots, j_l}^k, & 1 \leq l \leq M. \end{cases}$$

Calculate $B_{j_1, \dots, j_M}^{l,P}$ ($l = 0, \dots, M$) by starting with $B_{j_1, \dots, j_M}^{0,P}$ as the initial matrix. Furthermore, calculate

$$\begin{aligned} L_{j_1, \dots, j_M}^M &= B_{j_1, \dots, j_M}^{M,P} \circ T_\gamma(S_{j_1, \dots, j_M}^P, S_{j_1, \dots, j_M}), \\ C_M(S_{j_1, \dots, j_M}^P, S_{j_1, \dots, j_M}^P) &= C_0(S_{j_1, \dots, j_M}^P, S_{j_1, \dots, j_M}^P) \\ &\quad - \sum_{k=0}^{M-1} B_{j_1, \dots, j_M}^{k,P} \Phi_{j_1, \dots, j_k}^\top \widehat{K}_{j_1, \dots, j_k}^k \Phi_{j_1, \dots, j_k} B_{j_1, \dots, j_M}^{k,P^\top}, \\ V_{j_1, \dots, j_M}^{M,P} &= C_M(S_{j_1, \dots, j_M}^P, S_{j_1, \dots, j_M}^P) \circ T_\gamma(S_{j_1, \dots, j_M}^P, S_{j_1, \dots, j_M}^P). \end{aligned}$$

Step 3. Calculate $\widetilde{B}_{j_1, \dots, j_M}^{M,k} = B_{j_1, \dots, j_M}^{k,P} - L_{j_1, \dots, j_M}^M \Sigma_{j_1, \dots, j_M}^{-1} B_{j_1, \dots, j_M}^k$ ($0 \leq k < M$).

Step 4. For $0 \leq k < l < M$, it follows that

$$\widetilde{B}_{j_1, \dots, j_M}^{l,k} = \widetilde{B}_{j_1, \dots, j_M}^{l+1,k} - \widetilde{B}_{j_1, \dots, j_M}^{l+1,l} \Phi_{j_1, \dots, j_l}^\top \widehat{K}_{j_1, \dots, j_l}^l \Phi_{j_1, \dots, j_l} A_{j_1, \dots, j_l}^{l,k}, \quad (19)$$

where $A_{j_1, \dots, j_l}^{l,k} = A_{j_1, \dots, j_l}^{k,l^\top}$. Calculate $\widetilde{B}_{j_1, \dots, j_M}^{l,k}$ ($0 \leq k < l < M$) by using (19) recursively from $\widetilde{B}_{j_1, \dots, j_M}^{M,k}$ in Step 3 as the initial matrix.

Step 5. Calculate

$$\begin{aligned} \Psi_{j_1, \dots, j_M}^0 &= V_{j_1, \dots, j_M}^{M,P} - L_{j_1, \dots, j_M}^M \Sigma_{j_1, \dots, j_M}^{-1} L_{j_1, \dots, j_M}^{M^\top} \\ &\quad + \sum_{k=0}^{M-1} \widetilde{B}_{j_1, \dots, j_M}^{k+1,k} \Phi_{j_1, \dots, j_k}^\top \widehat{K}_{j_1, \dots, j_k}^k \Phi_{j_1, \dots, j_k} \widetilde{B}_{j_1, \dots, j_M}^{k+1,k^\top}. \end{aligned}$$

Step 6. Conduct the procedure of Steps 4 and 5 in Algorithm 3 and calculate $\omega_{j_1, \dots, j_m}^m$ ($m = M-1, \dots, 0$) for the fixed (j_1, \dots, j_M) .

Step 7. Calculate

$$\begin{aligned} \boldsymbol{\mu}_{j_1, \dots, j_M}^0 &= L_{j_1, \dots, j_M}^M \Sigma_{j_1, \dots, j_M}^{-1} \mathbf{Z}(S_{j_1, \dots, j_M}) \\ &\quad + \sum_{k=0}^{M-1} \widetilde{B}_{j_1, \dots, j_M}^{k+1,k} \Phi_{j_1, \dots, j_k}^\top \widehat{K}_{j_1, \dots, j_k}^k \Phi_{j_1, \dots, j_k} \omega_{j_1, \dots, j_k}^k. \end{aligned}$$

Step 8. Output $\boldsymbol{\mu}_{j_1, \dots, j_M}^0$ and Ψ_{j_1, \dots, j_M}^0 .

Therefore, we can obtain (17) and (18) from only Algorithm 4 without Algorithm 1. In steps except for Steps 5, 7, and 8 of Algorithm 4, we calculate the matrices required to obtain $\boldsymbol{\mu}_{j_1, \dots, j_M}^0$ and Ψ_{j_1, \dots, j_M}^0 . Note that if $M = 1$, then (19) and calculations corresponding

to (12) and (14) of Algorithm 3 are unnecessary. Similar to Algorithm 3, all of $A_{j_1, \dots, j_m}^{k,l}$ ($0 \leq k \leq l \leq m$, $m = M-1, \dots, 0$) calculated in Step 1 of Algorithm 4 are not necessarily used in the subsequent steps.

We can efficiently implement Algorithm 4 because this algorithm includes not the inverse of an $n \times n$ matrix but the inverse of the $|S_{j_1, \dots, j_M}| \times |S_{j_1, \dots, j_M}|$ sparse matrices Σ_{j_1, \dots, j_M} and $r_{j_1, \dots, j_m} \times r_{j_1, \dots, j_m}$ matrices ($r_{j_1, \dots, j_m} \ll n$), similar to Algorithm 3.

For the operation count and storage of Algorithm 4, we assume $|S_{j_1, \dots, j_M}^P| = O(r)$ as well as the assumptions required in the derivation of the time and memory complexity of Algorithm 3. Note that these assumptions are available only in the discussion on the complexities. By an argument similar to the case of Algorithm 3, for the fixed index (j_1, \dots, j_M) of S_{j_1, \dots, j_M}^P , we find that Algorithm 4 does not require $O(n^3)$ operations and $O(n^2)$ memory. Consequently, the M -RA-lp can handle massive spatial datasets such that the original model is computationally infeasible as shown in the fourth simulation of Section 5.1.

Similar to Algorithm 3, Algorithm 4 can also be parallelized except for a part of Steps 1 and 2. In particular, Algorithm 4 provides $\boldsymbol{\mu}_{j_1, \dots, j_M}^0$ and Ψ_{j_1, \dots, j_M}^0 only for the fixed index (j_1, \dots, j_M) , while its parallel version can calculate those for any (j_1, \dots, j_M) in parallel (see Algorithm 6 in Appendix D.2).

4.3 Relationship with the MLP and M -RA

First, we compare the M -RA-lp to the MLP proposed by Hirano (2017). From the viewpoint of the M -RA-lp, the MLP carries out the M -RA-lp with $M = 1$, $Q_0 = S_0$, and $J_1 = 1$ ($D_0 = D_1$) in Algorithm 1. In this sense, we regard the M -RA-lp as an extension of the MLP. The approximated covariance matrix by the MLP is given by

$$\begin{aligned} C_{\text{MLP}}(S_0, S_0) &= C_{\tau_0}(S_0, S_0) + \{C_0(S_0, S_0) - C_{\tau_0}(S_0, S_0)\} \circ T_\gamma(S_0, S_0) \\ &= B_0^0 \Phi_0^\top \hat{K}_0^0 \Phi_0 B_0^{0\top} + C_{\text{sparse}}(S_0, S_0), \end{aligned} \quad (20)$$

where $C_{\text{sparse}}(S_0, S_0) = \{C_0(S_0, S_0) - C_{\tau_0}(S_0, S_0)\} \circ T_\gamma(S_0, S_0)$ is the sparse matrix, and Φ_0 is obtained by using Algorithm 2. Since $C_0(S_0, S_0)$ in (1) and (2) is replaced with $C_{\text{MLP}}(S_0, S_0)$ in the estimation and prediction by the MLP, the inverse matrix and determinant of $C_{\text{MLP}}(S_0, S_0) + \tau^2 \mathbf{I}_n$ need to be calculated efficiently. As described in Hirano (2017), their calculations are achieved by using

$$\begin{aligned} \{C_{\text{MLP}}(S_0, S_0) + \tau^2 \mathbf{I}_n\}^{-1} &= \{C_{\text{sparse}}(S_0, S_0) + \tau^2 \mathbf{I}_n\}^{-1} \\ &\quad - \{C_{\text{sparse}}(S_0, S_0) + \tau^2 \mathbf{I}_n\}^{-1} B_0^0 \Phi_0^\top \left[\hat{K}_0^{0^{-1}} + \Phi_0 B_0^{0\top} \{C_{\text{sparse}}(S_0, S_0) + \tau^2 \mathbf{I}_n\}^{-1} \right. \\ &\quad \times \left. B_0^0 \Phi_0^\top \right]^{-1} \Phi_0 B_0^{0\top} \{C_{\text{sparse}}(S_0, S_0) + \tau^2 \mathbf{I}_n\}^{-1} \end{aligned}$$

and

$$\begin{aligned} \det \{C_{\text{MLP}}(S_0, S_0) + \tau^2 \mathbf{I}_n\} &= \det \{C_{\text{sparse}}(S_0, S_0) + \tau^2 \mathbf{I}_n\} \det (\hat{K}_0^0) \\ &\times \det \left[\hat{K}_0^{0^{-1}} + \Phi_0 B_0^{0\top} \{C_{\text{sparse}}(S_0, S_0) + \tau^2 \mathbf{I}_n\}^{-1} B_0^0 \Phi_0^\top \right]. \end{aligned}$$

These expansions are derived from Theorems 18.1.1 and 18.2.8 of Harville (1997), and we can treat them rapidly because they contain only the inverse matrix and determinant of the $n \times n$ sparse matrix $C_{\text{sparse}}(S_0, S_0) + \tau^2 \mathbf{I}_n$ and $r_0 \times r_0$ matrices.

In comparison with (6), (20) includes only the linear projection term at resolution 0, whereas the M -RA-lp has the additional linear projection terms at higher resolutions. Since the linear projection at resolution 0 focuses on fitting the large-scale dependence structure, a modification is required to capture the small-scale spatial variations (see Hirano, 2017). The second term in (20) shows the modification of the linear projection through the covariance tapering. Although the modification in the MLP is conducted on the whole region D_0 , this type of the modification in the M -RA-lp corresponds to the last term in (6) and is conducted on each subregion D_{j_1, \dots, j_M} to elicit Algorithms 3 and 4. However, the overall modification of the M -RA-lp by adding the linear projection terms at higher resolutions can more accurately approximate the small-scale dependence structure than that of the MLP (see Figure 1 for details).

Second, we explain the relationship between the M -RA-lp and the M -RA. In Algorithms 1, 3, and 4, if we set $\Phi_{j_1, \dots, j_m} = \mathbf{I}_{|Q_{j_1, \dots, j_m}|}$ and $T_\gamma(\mathbf{s}_1, \mathbf{s}_2) = 1$, the M -RA-lp is identical with the M -RA. In this sense, the M -RA-lp is regarded as an extension of the M -RA. Unlike Proposition 1 (d), the approximated covariance function by the M -RA equals the original covariance function if the two locations belong to D_{j_1, \dots, j_M} because $T_\gamma(\mathbf{s}_1, \mathbf{s}_2) = 1$ (see Section 2.4.5 of Katzfuss, 2017). However, from $\Phi_{j_1, \dots, j_m} = \mathbf{I}_{|Q_{j_1, \dots, j_m}|}$, it might be necessary to pay attention to the knot selection.

Furthermore, the introduction of Φ_{j_1, \dots, j_m} can yield the stable numerical calculation. In several steps of Algorithms 3 and 4, we conduct the calculation related to the inverse matrix of $\hat{K}_{j_1, \dots, j_m}^{m-1} = \Phi_{j_1, \dots, j_m} K_{j_1, \dots, j_m}^m \Phi_{j_1, \dots, j_m}^\top$ ($m = 0, \dots, M-1$). If a positive definite matrix is ill-conditioned, the calculation of the inverse matrix may be unstable with the propagation of round-off errors due to the finite precision arithmetic. How well the positive definite matrix is conditioned can be evaluated by the condition number σ_l/σ_s which means the ratio of the largest σ_l and the smallest σ_s eigenvalues of the positive definite matrix (see Dixon, 1983). The condition number closer to 1 indicates better numerical stability. The following simulation is similar to the one in Section 3.2 of Banerjee et al. (2013) and empirically shows the smaller condition number of $\hat{K}_{j_1, \dots, j_m}^{m-1}$ in the M -RA-lp over the M -RA.

Table 1: Comparative performance of the M -RA and M -RA-lp with respect to the logarithmic transformation of the condition number in $C_0(\mathbf{s}_1, \mathbf{s}_2) = \exp(-5\|\mathbf{s}_1 - \mathbf{s}_2\|)$.

n	Approximation	Rank	$\widehat{K}_0^{0^{-1}}$	$\widehat{K}_1^{1^{-1}}$	$\widehat{K}_{1,1}^{2^{-1}}$	$\widehat{K}_{1,1,1}^{3^{-1}}$	$\widehat{K}_{1,1,1,1}^{4^{-1}}$
5,000	M -RA	5	2.7457×10^{-12}	4.1968×10^{-8}	2.3786×10^{-4}	4.7041×10^{-4}	0.8624
		10	0.0035	1.7480×10^{-4}	0.0040	1.8454	3.4786
		15	2.3175×10^{-4}	0.0048	4.5554×10^{-4}	2.8131	4.4041
	M -RA-lp	5	4.2507×10^{-4}	0.0031	0.0168	0.0154	0.0691
		10	0.0248	0.0760	0.0391	0.0604	0.2241
		15	0.0592	0.1244	0.1417	0.2650	0.5392
10,000	M -RA	5	1.0819×10^{-10}	4.0632×10^{-11}	7.8879×10^{-7}	0.0440	8.0198×10^{-5}
		10	0.0033	6.6363×10^{-7}	9.3172×10^{-4}	1.8893	3.5504
		15	4.5924×10^{-6}	3.2506×10^{-9}	0.0038	0.0999	7.1757
	M -RA-lp	5	0.0305	0.0069	0.0380	0.0261	0.0097
		10	0.0545	0.0772	0.0366	0.0595	0.1512
		15	0.1070	0.0879	0.1072	0.1564	0.2817

Table 2: Comparative performance of the M -RA and M -RA-lp with respect to the logarithmic transformation of the condition number in $C_0(\mathbf{s}_1, \mathbf{s}_2) = \exp(-2.5(\|\mathbf{s}_1 - \mathbf{s}_2\|/10^2)^2)$.

n	Approximation	Rank	$\widehat{K}_0^{0^{-1}}$	$\widehat{K}_1^{1^{-1}}$	$\widehat{K}_{1,1}^{2^{-1}}$	$\widehat{K}_{1,1,1}^{3^{-1}}$	$\widehat{K}_{1,1,1,1}^{4^{-1}}$
5,000	M -RA	5	4.7199	7.6432	8.2238	9.2433	9.4813
		10	9.8629	12.0785	15.9587	16.4546	14.3746
		15	12.6046	16.9184	18.7201	15.4269	16.7445
	M -RA-lp	5	3.2443	2.6734	2.7241	3.4194	4.2966
		10	5.8569	4.8034	6.8916	7.2595	8.0247
		15	8.2005	6.9981	7.6940	10.2207	12.2585
10,000	M -RA	5	5.3286	7.3821	7.8050	9.3527	10.6376
		10	10.6290	12.4498	14.0487	14.2829	13.4687
		15	14.0862	17.2333	18.7836	15.6605	17.5230
	M -RA-lp	5	4.3762	3.4216	3.5816	4.8419	4.8598
		10	6.6606	5.9712	4.0011	7.5025	7.9609
		15	7.5037	7.9213	6.6500	9.9056	11.8865

We consider $M = 5$ and the two covariance functions, that is, the exponential covariance function $C_0(\mathbf{s}_1, \mathbf{s}_2) = \exp(-5\|\mathbf{s}_1 - \mathbf{s}_2\|)$ and the Gaussian covariance function $C_0(\mathbf{s}_1, \mathbf{s}_2) = \exp(-2.5(\|\mathbf{s}_1 - \mathbf{s}_2\|/10^2)^2)$, generate locations in $[0, 100]^2$ uniformly, and evaluate the average value of the logarithmic transformation of the condition numbers of $\widehat{K}_{1,\dots,1}^{m^{-1}}$ ($m = 0, \dots, 4$) for the ten datasets. Each domain is divided into two equal subregions, that is, $J_1 = \dots = J_5 = 2$. In the M -RA-lp, the sizes of Q_{j_1,\dots,j_m} were 300, 100, 50, 30, and 20 for $m = 0, \dots, 4$, respectively, and we selected Φ_{j_1,\dots,j_m} such that Algorithm 2 almost achieved some target values of the rank.

Tables 1 and 2 illustrate the comparison of the condition numbers between the M -RA and the M -RA-lp. Rank in Tables 1 and 2 means the target value of the rank of Φ_{j_1,\dots,j_m} in the M -RA-lp and the size of Q_{j_1,\dots,j_m} in the M -RA. From Tables 1 and

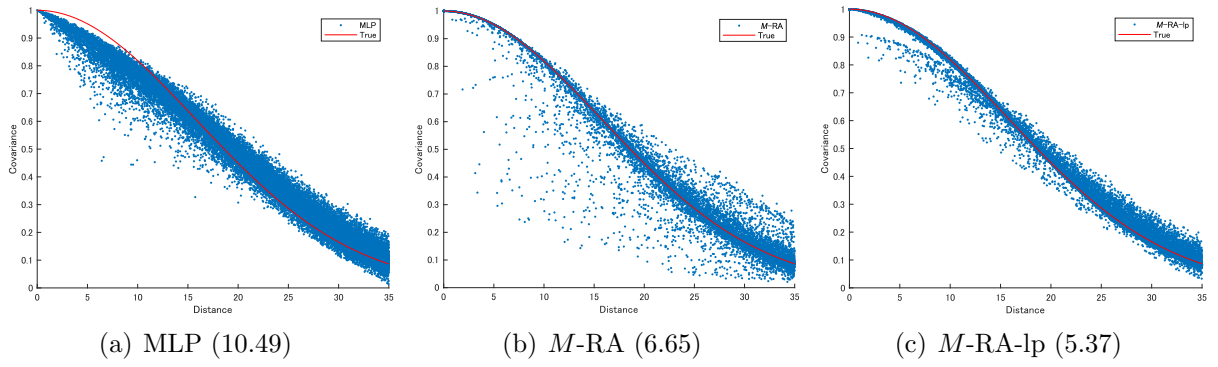


Figure 1: $C_0(\mathbf{s}_1, \mathbf{s}_2) = \exp(-0.002\|\mathbf{s}_1 - \mathbf{s}_2\|^2)$ (solid line) and its three approximations (points). 500 random locations are uniformly generated in $[0, 100]^2$. We set $\gamma = 10$, $M = 2$, and $J_1 = J_2 = 2$, and each domain is divided into equal subregions. The Frobenius norms of the difference between the true covariance matrix and the approximated one are given within parenthesis. (a) MLP. The selected rank of Φ_0 in Algorithm 2 was 15. (b) M -RA with $|Q_j| = 16$ ($j = 0, 1, 2$). (c) M -RA-lp with $Q_j = S_j$ ($j = 0, 1, 2$). The selected ranks of Φ_j ($j = 0, 1, 2$) in Algorithm 2 were 16, 14, and 15.

2, as the resolution and/or rank increased, the condition number tended to increase. Moreover, the smoothness of $C_0(\mathbf{s}_1, \mathbf{s}_2) = \exp(-2.5(\|\mathbf{s}_1 - \mathbf{s}_2\|/10^2)^2)$ caused the larger condition numbers as a whole. The condition numbers of the M -RA-lp were holistically smaller than those of the M -RA in similar situations. This may be because the M -RA-lp replaces the predictive process in the M -RA with the linear projection. Section 3.2 of Banerjee et al. (2013) empirically showed the smaller condition number of the covariance matrix approximated by the linear projection than that by the predictive process. We also obtained similar results for different types of partitions and covariance functions, but these are not reported here.

Unlike the M -RA, the M -RA-lp needs to implement Algorithm 2 for each subregion except for the one at the highest resolution. Although Algorithm 2 is implemented quickly, large M and J_i ($i = 1, \dots, M-1$) cause the unignorable computational cost due to a large number of implementations of Algorithm 2. Therefore, we typically select low M and J_i ($i = 1, \dots, M-1$) in the M -RA-lp compared to the M -RA, but the size of Σ_{j_1, \dots, j_M} is likely to become large and make it difficult computationally to conduct the calculation related to the inverse of Σ_{j_1, \dots, j_M} in Algorithms 3 and 4. To avoid this problem, we introduce T_γ in Step 4 of Algorithm 1 and make Σ_{j_1, \dots, j_M} sparse unlike the M -RA. If we need large M and J_i in order to bypass the lack of memory, the total computational time of Algorithm 2 can be shortened by selecting small $|Q_{j_1, \dots, j_m}|$ and r_{j_1, \dots, j_m} .

Figure 1 describes the typical characteristics of the three approximation methods for the original covariance function. The fitting of the MLP to the original covariance function

was worse around the origin than that of the M -RA-lp. This suggests that the modification by the covariance tapering on the whole spatial region can be insufficient unlike the linear projection at higher resolutions plus the modification by the covariance tapering on each subregion when the small-scale spatial correlation has smoothness such as the Gaussian covariance function. The M -RA-lp showed the best approximation accuracy with regard to the Frobenius norm. However, Figure 1 (c) represents the partly mismatched fitting of the M -RA-lp around the origin because the approximation procedure of Algorithm 1 stops in the early stages if the two locations are not in the same subregion at the low resolution. This problem can also occur in the M -RA. A taper version of the M -RA-lp based on Katzfuss and Gong (2019) may resolve this artificiality.

5 Illustrations

In this section, we compare our proposed M -RA-lp with the MLP and M -RA by using the simulated and real data. All computations were carried out by using MATLAB on a single core machine (4.20 GHz) with 64 GB RAM. For sparse matrix calculations and the optimization of the log-likelihood function, we used the MATLAB functions `sparse` and `fmincon`, respectively.

5.1 Simulation study

We evaluated the performance of Algorithms 3 and 4 in our proposed M -RA-lp through simulation studies. Let $D_0 = [0, 100]^2$ be the sampling domain, and observed locations were sampled from a uniform distribution over D_0 . We considered the zero-mean Gaussian processes having the same covariance functions as those in simulations of Tables 1 and 2 of Section 4.3. When pairs of observations were more than 0.6 unit distant from each other in the case of the exponential covariance function, they had negligible (< 0.05) correlation. This distance is called the effective range, and 0.6 unit represents the Gaussian process with the weak spatial correlation. In contrast, the effective range in the case of the Gaussian covariance function was 110 unit, and it shows the strong spatial correlation. The measurement error variance τ^2 was 0.5. In this subsection, we set $|Q_{j_1, \dots, j_m}| = r$ ($m = 0, \dots, M - 1$) in the M -RA and $J_i = J$ ($i = 1, \dots, M$) except for the fourth simulation, and the equal-area partitions were chosen when the resolution increased. The average value of total computational times required for one calculation of the evaluation measure in each iteration was recorded and scaled relative to that of the original model except for the fourth simulation.

First, we compared the approximation accuracy of the original log-likelihood function

Table 3: Comparison of the log-score.

		Covariance	Original model			M -RA-lp		
						5	10	20
log-score ($\times 10^4$)	Exponential		-1.6148			-1.6159	-1.6155	-1.6153
	Gaussian		-1.0763			-1.0777	-1.0769	-1.0764
Relative time			1			0.2609	0.2640	0.2689
		Covariance	MLP			M -RA		
			10	20	40	M=2	M=4	M=5
log-score ($\times 10^4$)	Exponential	-1.6156	-1.6154	-1.6151	-1.6162	-1.6157	-1.6155	
	Gaussian	-1.0773	-1.0770	-1.0765	-1.0799	-1.0774	-1.0770	
Relative time		0.5142	0.6813	0.9658	0.2318	0.2620	0.2824	

Three cases in the *M*-RA-lp and MLP represent target values of r_j 's and r_0 , respectively.

in Algorithm 3 of the *M*-RA-lp with those of the MLP and *M*-RA. All comparisons were conducted based on the log-score which is defined by the log-likelihood function at the true parameter values. The log-score indicates how well the original covariance function is approximated. Since this measure is maximized in the sense of the expectation by the original model (see, e.g., Gneiting and Katzfuss, 2014), the log-score by the original covariance function is expected to have the highest value on average. Thus, the higher log-score is better.

For a fixed configuration of 10,000 sampling locations, we calculated the sample mean of the log-scores of 50 simulations. This procedure was iterated 10 times, and we recorded their average value. For the *M*-RA-lp with $\gamma = 1$ and $M = 2$, we set $|Q_0| = 300$, $|Q_1| = |Q_2| = 100$, and $J = 2$. In Algorithm 2, we selected each ε such that all of r_j ($j = 0, 1, 2$) over the iterations were nearly equal to the target values of 5, 10, and 20. For the MLP with $\gamma = 1$, the target values of r_0 were 10, 20, and 40. For the *M*-RA with $r = 10$ and $M = 2, 4, 5$, we selected J that almost satisfies $r = n / (J^M)$. This selection guideline $r = n / (J^M)$ was often used in simulation studies of Katzfuss (2017).

The results are summarized in Table 3. We compared the three approximation methods on the basis of the *M*-RA-lp with r_j ($j = 0, 1, 2$) nearly equal to 10. The comparison of these methods showed common characteristics in both covariance functions. The MLP eventually indicated a similar log-score and larger computational time in $r_0 \approx 20$. Unlike the case of the Gaussian covariance function, the log-score of the MLP in the case of the exponential covariance function was better slightly in the sense of the magnitude relationship with those of the *M*-RA-lp and *M*-RA. This is because the exponential covariance function in this simulation has the weak spatial correlation and the modification by the covariance tapering works well. For the *M*-RA with $M = 2$, although the computational

Table 4: Comparison of the MSPE and CRPS.

Covariance		Original model	<i>M</i> -RA-lp		
			5	10	20
MSPE	Exponential	0.9300	0.9931	0.9771	0.9660
	Gaussian	0.0056	0.0094	0.0062	0.0058
CRPS	Exponential	0.5351	0.5609	0.5529	0.5478
	Gaussian	0.0423	0.0542	0.0447	0.0429
Relative time		1	0.4830	0.4879	0.4952

Covariance		MLP			<i>M</i> -RA		
		10	20	40	M=2	M=4	M=5
MSPE	Exponential	0.9694	0.9501	0.9385	1.0572	0.9969	0.9728
	Gaussian	0.0139	0.0064	0.0059	0.0162	0.0074	0.0067
CRPS	Exponential	0.5570	0.5479	0.5417	0.5814	0.5642	0.5570
	Gaussian	0.0656	0.0452	0.0433	0.0716	0.0486	0.0464
Relative time		0.7656	0.8936	1.2989	0.4403	0.5035	0.5339

Three cases in the *M*-RA-lp and MLP represent target values of r_j 's and r_0 , respectively.

time was lower, the log-score was not good. In the case of $M = 5$, the log-score was similar to that of the *M*-RA-lp, but the computational time was somewhat large. Also, in other cases, the log-scores and computational times of the *M*-RA-lp were not improved simultaneously compared with those of the MLP and *M*-RA. These results support the effectiveness of the *M*-RA-lp for efficiently approximating the log-likelihood function.

Second, we assessed the prediction performance of Algorithm 4 with regard to the mean squared prediction error (MSPE) and the continuous ranked probability score (CRPS). The CRPS evaluates the fitting of the predictive distribution to the data (see Gneiting and Raftery, 2007; Gneiting and Katzfuss, 2014). The lower MSPE and CRPS are better. The prediction point was $(1, 1)^\top$. The tuning parameter settings in the three approximation methods and the iteration procedure were the same as those in the first simulation except that the MSPE and averaged CRPS were calculated from 100 simulations.

The characteristics of the results in Table 4 were similar to those of the first simulation. The weak spatial correlation in the case of the exponential covariance function gave rise to the better prediction accuracy of the MLP than that of the *M*-RA-lp in many cases because of the effective modification of the covariance tapering. However, the computational time of the MLP is larger than that of the *M*-RA-lp, and the prediction accuracy of the MLP in the case of the Gaussian covariance function degrades due to the strong spatial correlation unlike the *M*-RA-lp. Moreover, for the Gaussian covariance function, the *M*-RA-lp with r_j ($j = 0, 1, 2$) nearly equal to 20 showed almost the same MSPE and CRPS as those of the original model despite half the computational time. These results

demonstrate that the M -RA-lp can achieve better prediction accuracy rapidly than the MLP and M -RA.

Through the first and second simulations in Section 5.1, we examined the effect of the covariance tapering in Σ_{j_1, \dots, j_M} . The averaged percentage of non-zero entries in Σ_{j_1, \dots, j_M} , that is, the averaged sparsity of Σ_{j_1, \dots, j_M} , was 0.16%. In the case where the covariance tapering was not used in Σ_{j_1, \dots, j_M} of the M -RA-lp, the relative computational times in the first simulation were 0.3123, 0.3154, and 0.3193 for r_j ($j = 0, 1, 2$) nearly equal to 5, 10, and 20, respectively. Similarly, the ones in the second simulation were 0.5783, 0.5832, and 0.5891 for r_j ($j = 0, 1, 2$) nearly equal to 5, 10, and 20, respectively. Thus, the covariance tapering reduced the computational time by approximately 19% in the first and second simulations. On the other hand, in the case of the exponential covariance function, the relative Frobenius norms between the original covariance matrix and the approximated covariance matrix by the M -RA-lp without the covariance tapering, which were scaled relative to $\|C_0(S_0, S_0) - C_{M\text{-RA-lp}}(S_0, S_0)\|_F$, were 0.7748, 0.7989, and 0.8100 for r_j ($j = 0, 1, 2$) nearly equal to 5, 10, and 20, respectively. As r_j 's increase, the M -RA-lp improves the approximation of the small-scale spatial variations of the original covariance function. Consequently, since the effect of the covariance tapering decreases, the relative Frobenius norm is closer to 1. Considering that the averaged sparsity was 0.16%, the reduction of the approximation accuracy for the original covariance matrix by using the covariance tapering was small. This is because the spatial correlation in this case was weak and the covariance tapering worked well. In the case of the Gaussian covariance function, the relative Frobenius norms were 0.9989, 0.9998, and 0.9998 for r_j ($j = 0, 1, 2$) nearly equal to 5, 10, and 20, respectively. In this case, since the small-scale spatial variations of the original covariance function are well approximated by the M -RA-lp up to resolution $m = 1$ in Algorithm 1 with $M = 2$, the reduction of the approximation accuracy by the covariance tapering was very small. As a consequence, it is suggested that the covariance tapering in the M -RA-lp reduced the computational time efficiently in the first and second simulations.

Third, we investigated scalability of the M -RA-lp. The sample size n was selected from 5,000 to 20,000, and the count of iterations for calculating the averaged total computational time of one log-score, MSPE, and CRPS by Algorithms 3 and 4 was 3. However, for $n = 10,000$, we used the summation of the computational times in Tables 3 and 4. We employed tuning parameter settings under which the three approximation methods showed almost the same prediction accuracy for $n = 10,000$ in the second simulation. Specifically, all of r_j ($j = 0, 1, 2$) of the M -RA-lp were nearly equal to 10, and r_0 of the MLP was almost 20. For the M -RA, we set $r = 10$, $M = 5$, and $J = 4$ for $n = 10,000$

Table 5: Comparison of the computational time.

	$n = 5,000$	$n = 10,000$	$n = 15,000$	$n = 20,000$
Original model	1	1	1	1
M -RA-lp	0.5558	0.3669	0.3628	0.3236
MLP	1.1347	0.7788	0.6870	0.6722
M -RA	0.6275	0.3979	0.3512	0.3003

and selected M to almost satisfy $r = n / (J^M)$ as $r = 10$ and $J = 4$ for different values of n .

Table 5 displays better scalability of the M -RA-lp and M -RA than that of the MLP, and the M -RA showed a shorter computational time than that of the M -RA-lp for very large n . This is because the M -RA-lp requires the additional computational time by Algorithm 2 and matrix multiplication related to Φ_j ($j = 0, 1, 2$). The third simulation indicates that the M -RA has competitive scalability. However, from the results in Tables 1–4, we believe that the M -RA-lp can attain a better and stable inference by the somewhat additional computational time.

Fourth, we examined computational feasibility of the M -RA-lp when $n = 10^5$ or more. These kinds of massive spatial datasets are often obtained by sensing devices on satellites. For $n = 100,000, 120,000$, we recorded the averaged total computational time of one log-score, MSPE, and CRPS by Algorithms 3 and 4 from the three iterations. In this case, it was necessary to pay attention to the memory burden as well as the expensive computational cost. Since the original model and MLP require the $n \times n$ covariance matrix, we experienced the lack of memory. Similarly, the M -RA-lp with $M = 2$, $(J_1, J_2) = (2, 2)$, $(|Q_0|, |Q_{j_1}|) = (300, 100)$ ($1 \leq j_1 \leq 2$), $\gamma = 1$ used in the third simulation also caused the lack of memory due to large $|S_{j_1, \dots, j_M}|$. Hence, we needed to increase M and/or J_i in order to reduce the size of S_{j_1, \dots, j_M} . Specifically, for the M -RA-lp, we considered two cases: $M = 2$, $(J_1, J_2) = (2, 16)$, $(|Q_0|, |Q_{j_1}|) = (300, 100)$ ($1 \leq j_1 \leq 2$) and $M = 4$, $(J_1, J_2, J_3, J_4) = (2, 2, 8, 16)$, $(|Q_0|, |Q_{j_1}|, |Q_{j_1, j_2}|, |Q_{j_1, j_2, j_3}|) = (300, 100, 50, 30)$ ($1 \leq j_1 \leq 2, 1 \leq j_2 \leq 2, 1 \leq j_3 \leq 8$). For Cases 1 and 2, the target values of r_{j_1, \dots, j_m} 's were 10. Furthermore, we set the computational time of the M -RA with $M = 5$ and $J_i = J = 4$ ($i = 1, \dots, 5$) used in the third simulation as the baseline for calculating the relative time. For the M -RA, r was selected from $r = n / (J^M)$.

Table 6 shows the computational time for each method and suggests that it may be desirable to make both M and J_i large for the M -RA-lp in terms of the computational cost. Since the M -RA-lp with large M and/or J_i requires a large number of implementations of Algorithm 2, we selected relatively low $|Q_{j_1, \dots, j_m}|$ and r_{j_1, \dots, j_m} in spite of massive spatial

Table 6: Computational time for massive spatial datasets.

	M -RA	M -RA-lp (Case 1)	M -RA-lp (Case 2)
$n = 100,000$	1	1.0598	0.9327
$n = 120,000$	1	1.1047	0.9150

Case 1: $M = 2$, $(J_1, J_2) = (2, 16)$, $(|Q_0|, |Q_{j_1}|) = (300, 100)$; Case 2: $M = 4$, $(J_1, J_2, J_3, J_4) = (2, 2, 8, 16)$, $(|Q_0|, |Q_{j_1}|, |Q_{j_1, j_2}|, |Q_{j_1, j_2, j_3}|) = (300, 100, 50, 30)$.

datasets. This might lead to insufficient approximation of the small-scale spatial variation when the variation of the spatial correlation around the origin is smooth. Since the M -RA does not conduct Algorithm 2, we can select large M , J , and r . As a consequence, the M -RA can likely avoid this problem, but Tables 1 and 2 indicate that numerical instability might occur unlike the M -RA-lp.

5.2 Real data analysis

In this subsection, we applied our proposed M -RA-lp to the air dose rates, that is, the amount of radiation per unit time in the air. The data were created by using the results of the vehicle-borne survey conducted by the Nuclear Regulation Authority (NRA) from November 2 to December 18, 2015, and are available at <https://emdb.jaea.go.jp/emdb/en/portals/b1010202/>. In particular, we focused on the air dose rates in Chiba prefecture, and this dataset includes the air dose rates (microsievert per hour), longitudes, and latitudes at 39,553 sampling locations. Since they were observed on irregularly spaced locations at discrete time points, they were rigorously spatio-temporal data. However, we regarded the dataset as spatial data by assuming that the trend of the air dose rates does not fluctuate largely over a short period. Moreover, to satisfy the assumption of Gaussianity over the whole region, we selected 7,801 locations inside the rectangular region $[140.00, 140.15] \times [35.65, 35.87]$ and applied the logarithmic transformation to these air dose rates. Figure 2 shows an overview of the transformed data. After subtracting the sample mean from the transformed data, some exploratory analyses led us to use the zero-mean Gaussian process with an exponential covariance function $C_0(\mathbf{s}_1, \mathbf{s}_2) = \sigma^2 \exp(-\theta \|\mathbf{s}_1 - \mathbf{s}_2\|)$. Also, to check the predictive performance, we considered a test set of size 129 from 7,801 data points. The test set belonged to $[140.07, 140.08] \times [35.71, 35.74]$, and we designed the domain partitioning such that $[140.07, 140.08] \times [35.71, 35.74]$ was inside the subregion at the highest resolution.

First, we estimated the unknown parameters σ^2 , θ , and τ^2 by maximizing the approximated log-likelihood functions of the M -RA-lp, MLP, and M -RA. Then, we calculated

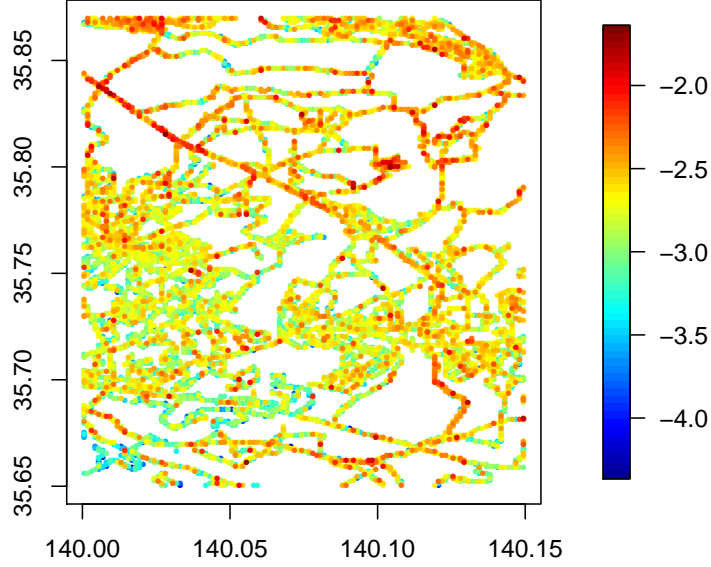


Figure 2: The logarithmic transformation of the air dose rates at 7,801 sampling locations in Chiba prefecture.

the predictive distribution of the test set to compare the three methods by assessing the MSPE and averaged CRPS. In order to calculate the two prediction measures, we adopted the predictive distribution $\mathbf{Z}(S_0^P) | \mathbf{Z}(S_0)$ instead of (2) because $\mathbf{Y}_0(S_0^P)$ is not observed. $\mathbf{Z}(S_0^P) | \mathbf{Z}(S_0)$ is given just by adding $\tau^2 \mathbf{I}_{n'}$ to the covariance matrix in (2).

We compared the M -RA-lp with $M = 2$ to the MLP and M -RA with $M = 4$. γ in T_γ was 1. For the M -RA-lp, we set $(J_1, J_2) = (2, 2)$, $|Q_0| = 140$, and $|Q_1| = |Q_2| = 60$. We implemented Algorithm 2 such that r_0 and r_{j_1} ($j_1 = 1, 2$) were nearly equal to the target values 20 and 10, respectively. In the same way, the target value of r_0 in the MLP was set as 20. The M -RA had $(J_1, J_2, J_3, J_4) = (2, 2, 8, 16)$ because a few partitions at low resolution often improve the approximation of the original covariance function by avoiding the early stop of Algorithm 1. For the number of knots, we considered two cases: $(|Q_0|, |Q_{j_1}|, |Q_{j_1, j_2}|, |Q_{j_1, j_2, j_3}|) = (20, 10, 5, 5), (20, 10, 800, 70)$ ($1 \leq j_1 \leq 2, 1 \leq j_2 \leq 2, 1 \leq j_3 \leq 8$).

The results of the real data analysis are shown in Table 7. The MLP and the M -RA (Case 1) showed the discrepancy from the results of the original model in terms of the maximum log-likelihood values and prediction measures. In particular, the computational time of the MLP was larger than that of the original model due to Algorithm 2. Additionally, the estimated value of θ in the M -RA (Case 1) was very small because the approximation of the small-scale spatial variation is insufficient due to the small $|Q_{j_1, j_2}|$ and $|Q_{j_1, j_2, j_3}|$. Although the M -RA-lp had almost the same r_0 and r_{j_1} as the corresponding rank and number of knots in the MLP and M -RA (Case 1), the M -RA-lp achieved results similar to the original model. Furthermore, the computational time of the M -RA-

Table 7: Results of the real data analysis.

	$\hat{\sigma}^2$	$\hat{\theta}$	$\hat{\tau}^2$	Relative time	loglik.	MSPE	CRPS
Original model	0.0416	1.6109	0.0581	1.0000	-1051.7	0.0690	0.1464
<i>M</i> -RA-lp	0.0429	1.6073	0.0609	0.6952	-1067.5	0.0691	0.1471
MLP	0.0445	1.6268	0.0598	1.6422	-1101.5	0.0701	0.1477
<i>M</i> -RA (Case 1)	0.0409	0.7126	0.0635	0.2740	-1119.1	0.0700	0.1499
<i>M</i> -RA (Case 2)	0.0424	1.6402	0.0574	0.8952	-1061.8	0.0691	0.1480

Case 1: $(|Q_0|, |Q_{j_1}|, |Q_{j_1, j_2}|, |Q_{j_1, j_2, j_3}|) = (20, 10, 5, 5)$; Case 2: $(|Q_0|, |Q_{j_1}|, |Q_{j_1, j_2}|, |Q_{j_1, j_2, j_3}|) = (20, 10, 800, 70)$; Relative time: relative time per likelihood function evaluation; loglik.: maximum log-likelihood value.

lp was smaller than that of the original model. By increasing the number of knots at higher resolutions in order to capture the small-scale spatial variation, the *M*-RA (Case 2) showed results close to the original model, while the *M*-RA-lp attained similar results in the shorter computational time. Therefore, it is suggested that the *M*-RA-lp can more rapidly realize results close to the original model compared with the *M*-RA.

Finally, we produced the prediction surfaces in the rectangular region $[140.07, 140.08] \times [35.71, 35.74]$ so as to examine how well the *M*-RA-lp, MLP, and *M*-RA perform in the prediction of a region. The prediction surfaces were generated by calculating the mean vector of the predictive distribution at 31×31 lattice points in $[140.07, 140.08] \times [35.71, 35.74]$ by using 7,801 observations with the test set of 129 observations. For σ^2 , θ , and τ^2 , we used the estimated values of each method in the results of Table 7, and tuning parameter settings were also identical to those in the real data analysis of Table 7.

Figure 3 shows the prediction surfaces of the original model and three approximation methods. The prediction surfaces of the *M*-RA-lp, MLP, and *M*-RA (Case 2) were similar to that of the original model. For $\hat{\theta} = 1.6109$ in the original model of Table 7, the effective range was 1.86 km, which shows the weak spatial correlation because the sides of the sampling region are 13.58 km and 24.41km. Consequently, the MLP depicted the good prediction surface because of the effectiveness of the covariance tapering. Also, some partial shapes in the prediction surface of the *M*-RA (Case 2) resembled those of the original model very well because the *M*-RA completely recovers the spatial correlation between observations in $[140.07, 140.08] \times [35.71, 35.74]$ as explained in Section 4.3. However, the relative computational times of producing the prediction surfaces were 0.2063, 1.0299, 0.0715, and 0.3287 for the *M*-RA-lp, MLP, *M*-RA (Case 1), and *M*-RA (Case 2), respectively. The *M*-RA-lp generated the prediction surface in a shorter computation time than the *M*-RA (Case 2), and this demonstrates that the *M*-RA-lp is the reasonable fast computation approach.

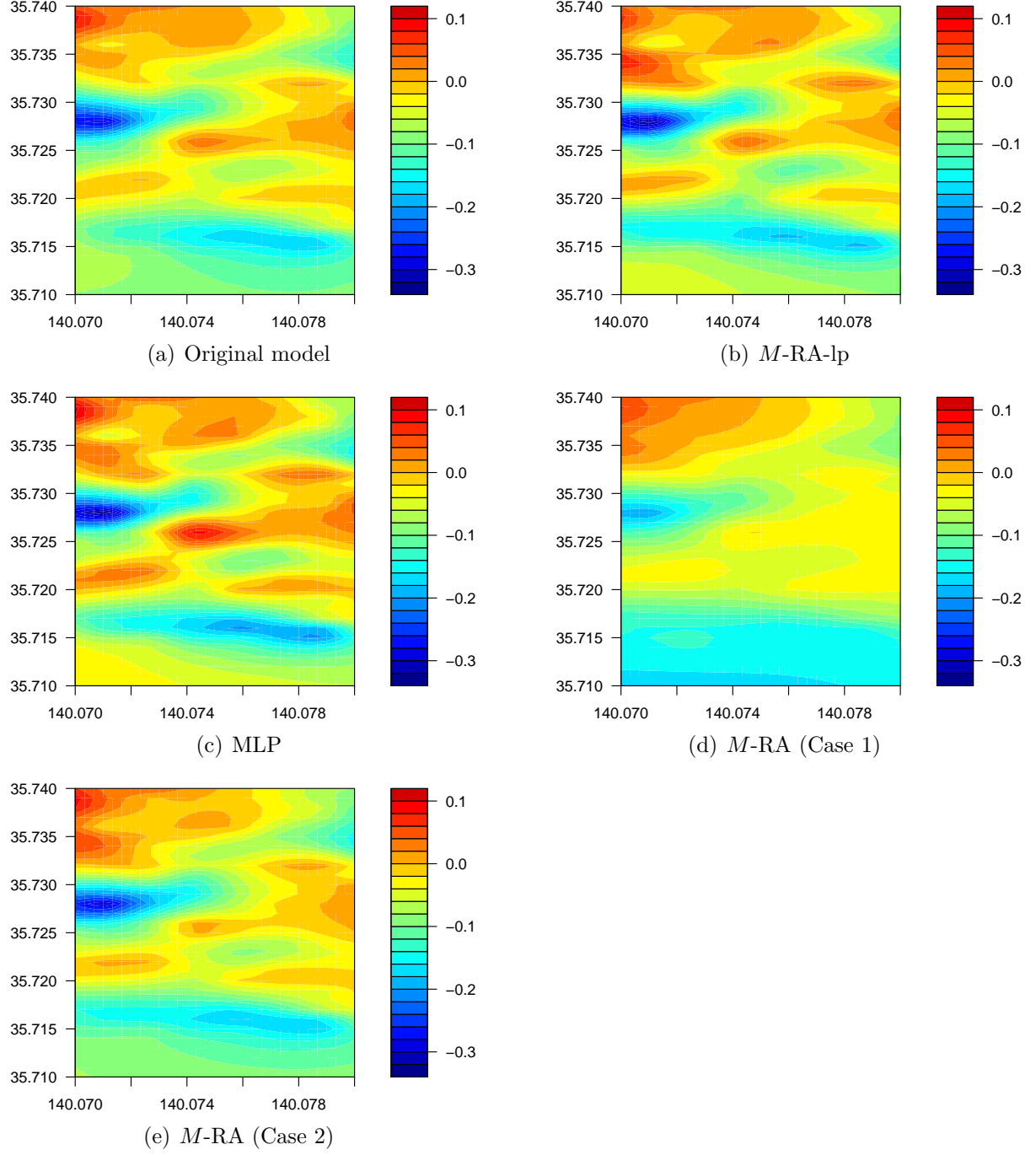


Figure 3: The prediction surfaces generated by the original model, M -RA-lp, MLP, and M -RA.

6 Conclusion and future studies

In this paper, we have described the multi-resolution approximation via linear projection (M -RA-lp). The proposed method refined the MLP of Hirano (2017) by introducing the multiple resolutions and the recursive partitioning of the entire spatial domain based on the idea of Katzfuss (2017). Also, the M -RA-lp can be regarded as an extension of the M -RA of Katzfuss (2017) by replacing the predictive process in the M -RA with the linear projection. Some simulations suggested that this replacement gave rise to better numerical stability by reducing the condition number, which is consistent with the results of Banerjee et al. (2013). In simulation studies and the real data analysis, the M -RA-lp was generally efficient compared with the MLP and M -RA in terms of the approximation of the log-likelihood function and predictive distribution at unobserved locations.

Some issues are to be solved in the future. First, Katzfuss and Gong (2019) pointed out discontinuities of the M -RA and proposed a taper version of the M -RA. In order to bypass the artificiality presented in Section 4.3, we plan to derive a taper version of the M -RA-lp. Second, since the M -RA-lp has many tuning parameters, a comprehensive study on their selection is left for a future study. The faster selection method of Φ_{j_1, \dots, j_m} should also be investigated. Third, Jurek and Katzfuss (2019) developed a multi-resolution filter for massive spatio-temporal data. Similarly, our proposed method might be extended to a spatio-temporal process. Finally, Katzfuss and Guinness (2020) proposed Vecchia approximations which contain many existing fast computation methods as well as the M -RA as special cases. This general Vecchia framework was applied to a variety of settings such as the prediction, non-Gaussian case, and computer experiments (Katzfuss et al., 2020a; Zilber and Katzfuss, 2020; Katzfuss et al., 2020b). It is also interesting to investigate the relationship between the Vecchia approximations and the M -RA-lp.

Appendix A Technical lemmas

This appendix collects some relevant results on matrix algebra.

Lemma A.1 (A part of Proposition 5.4 of Puntanen et al. (2011)). Let A be a positive semidefinite $n \times n$ matrix and B be an $n \times p$ matrix. If $\text{rank}(B) = p$ and $R(B) \cap R(A)^\perp = \{\mathbf{0}\}$, then $\text{rank}(B^\top AB) = p$.

Lemma A.2 (Lemma 2 of Welling (2010)). Let A be a positive definite $n \times n$ matrix, B be a positive definite $m \times m$ matrix, and C be a $m \times n$ matrix. Then,

$$(A^{-1} + C^\top B^{-1} C)^{-1} C^\top B^{-1} = AC^\top (CAC^\top + B)^{-1}.$$

We can prove Lemma A.2 by using Theorem 18.2.8 of Harville (1997) known as the Sherman–Morrison–Woodbury formula.

Appendix B Proof of Proposition 1

Proof of Proposition 1. (a) Consider $\mathbf{a}^\top C_m(S_0, S_0) \mathbf{a}$ for any $\mathbf{a} \in \mathbb{R}^n$ and any set of locations $S_0 \subset D_0$. We will show the assertion by mathematical induction in the same way as the proof of Proposition 1 of Katzfuss (2017). For $m = 1$, we have

$$\begin{aligned} C_0(S_0, S_0) - C_{\tau_0}(S_0, S_0) &= \text{Var}(\mathbf{Y}_0(S_0)) - \text{Var}(\boldsymbol{\tau}_0(S_0)) \\ &= \text{Var}(\mathbf{Y}_0(S_0)) - \text{Var}(E[\mathbf{Y}_0(S_0) | \Phi_0 \mathbf{Y}_0(Q_0)]) \\ &= \text{Var}(\mathbf{Y}_0(S_0) | \Phi_0 \mathbf{Y}_0(Q_0)), \end{aligned}$$

where the third equation holds by using the law of total variance, $Y_0(s) \sim \text{GP}(0, C_0)$, and the fact that $\text{Var}(\Phi_0 \mathbf{Y}_0(Q_0)) = \Phi_0 K_0^0 \Phi_0^\top$ is positive definite from the proof of Proposition 4.1 (a) of Hirano (2017). Thus, $C_0(S_0, S_0) - C_{\tau_0}(S_0, S_0)$ is positive semidefinite. For any $\mathbf{a} = (\mathbf{a}_1^\top, \dots, \mathbf{a}_{J_1}^\top)^\top \in \mathbb{R}^n$ such that $|\mathbf{a}_{j_1}| = |S_{j_1}|$ and $\mathbf{a}_{j_1} = \emptyset$ if $|S_{j_1}| = 0$,

$$\mathbf{a}^\top C_1(S_0, S_0) \mathbf{a} = \sum_{\substack{1 \leq j_1 \leq J_1, j_1 \notin A_1, \\ A_1 = \{j'_1 \mid |S_{j'_1}| = 0\}}} \mathbf{a}_{j_1}^\top \{C_0(S_{j_1}, S_{j_1}) - C_{\tau_0}(S_{j_1}, S_{j_1})\} \mathbf{a}_{j_1} \geq 0.$$

Therefore, the result holds for $m = 1$.

Next, assume that the result holds for $m = l$. Since $\text{rank}(\Phi_{j_1, \dots, j_l} K_{j_1, \dots, j_l}^l \Phi_{j_1, \dots, j_l}^\top) = r_{j_1, \dots, j_l}$ by the assumption and Lemma A.1, $\Phi_{j_1, \dots, j_l} K_{j_1, \dots, j_l}^l \Phi_{j_1, \dots, j_l}^\top$ is positive definite, so that $\Phi^{(l)} C_l(Q^{(l)}, Q^{(l)}) \Phi^{(l)\top}$ is also positive definite. Therefore, for $\delta_l(s) \sim \text{GP}(0, C_l)$, we can define

$$\begin{aligned} \tau_l(\mathbf{s}) &= E[\delta_l(\mathbf{s}) | \Phi^{(l)} \boldsymbol{\delta}_l(Q^{(l)})] \\ &= C_l(\mathbf{s}, Q^{(l)}) \Phi^{(l)\top} \left\{ \Phi^{(l)} C_l(Q^{(l)}, Q^{(l)}) \Phi^{(l)\top} \right\}^{-1} \Phi^{(l)} \boldsymbol{\delta}_l(Q^{(l)}). \end{aligned}$$

Then, in the same way as the argument of $m = 1$, $C_l(S_0, S_0) - C_{\tau_l}(S_0, S_0)$ is positive semidefinite because $C_l(S_0, S_0) - C_{\tau_l}(S_0, S_0) = \text{Var}(\boldsymbol{\delta}_l(S_0) | \Phi^{(l)} \boldsymbol{\delta}_l(Q^{(l)}))$.

Consider $m = l + 1$. For any $\mathbf{a} = (\mathbf{a}_{1, \dots, 1}^\top, \dots, \mathbf{a}_{J_1, \dots, J_{l+1}}^\top)^\top \in \mathbb{R}^n$ such that $|\mathbf{a}_{j_1, \dots, j_{l+1}}| = |S_{j_1, \dots, j_{l+1}}|$ and $\mathbf{a}_{j_1, \dots, j_{l+1}} = \emptyset$ if $|S_{j_1, \dots, j_{l+1}}| = 0$,

$$\begin{aligned} \mathbf{a}^\top C_{l+1}(S_0, S_0) \mathbf{a} &= \sum_{\substack{1 \leq j_1 \leq J_1, \dots, 1 \leq j_{l+1} \leq J_{l+1}, \\ (j_1, \dots, j_{l+1}) \notin A_{l+1}, \\ A_{l+1} = \{(j'_1, \dots, j'_{l+1}) \mid |S_{j'_1, \dots, j'_{l+1}}| = 0\}}} \mathbf{a}_{j_1, \dots, j_{l+1}}^\top \{C_l(S_{j_1, \dots, j_{l+1}}, S_{j_1, \dots, j_{l+1}}) \\ &\quad - C_{\tau_l}(S_{j_1, \dots, j_{l+1}}, S_{j_1, \dots, j_{l+1}})\} \mathbf{a}_{j_1, \dots, j_{l+1}} \\ &\geq 0. \end{aligned}$$

The result holds for $m = l + 1$. The proof is completed.

(b) As shown in the proof of Proposition 1 (a), $\Phi_0 K_0^0 \Phi_0^\top$ is positive definite. For $m = 1, \dots, M-1$, K_{j_1, \dots, j_m}^m is positive semidefinite from Proposition 1 (a). Since $\Phi_{j_1, \dots, j_m} K_{j_1, \dots, j_m}^m \Phi_{j_1, \dots, j_m}^\top$ is nonsingular by using Lemma A.1, $\Phi_{j_1, \dots, j_m} K_{j_1, \dots, j_m}^m \Phi_{j_1, \dots, j_m}^\top$ is positive definite.

(c) For any set of locations $S_0 \subset D_0$, we have

$$C_{M\text{-RA-lp}}(S_0, S_0) = \sum_{m=0}^{M-1} C_{\tau_m}(S_0, S_0) + C_M(S_0, S_0) \circ T_\gamma(S_0, S_0),$$

where $C_{\tau_m}(S_0, S_0)$ is the block diagonal matrix whose diagonal element is $B_{j_1, \dots, j_m}^m \Phi_{j_1, \dots, j_m}^\top \times \hat{K}_{j_1, \dots, j_m}^m \Phi_{j_1, \dots, j_m} B_{j_1, \dots, j_m}^{m\top}$ if $|S_{j_1, \dots, j_m}| \neq 0$. From Proposition 1 (b), $\hat{K}_{j_1, \dots, j_m}^m$ is positive definite, so that $C_{\tau_m}(S_0, S_0)$ is positive semidefinite. In addition, from Theorem 5.2.1 of Horn and Johnson (1991) and Proposition 1 (a), $C_M(S_0, S_0) \circ T_\gamma(S_0, S_0)$ is also positive semidefinite.

(d) Since \mathbf{s}_1 and \mathbf{s}_2 are always in the same subregion D_{j_1, \dots, j_m} at each m th resolution ($m = 0, \dots, M$),

$$C_{M\text{-RA-lp}}(\mathbf{s}_1, \mathbf{s}_2) = \sum_{m=0}^{M-1} C_{\tau_m}(\mathbf{s}_1, \mathbf{s}_2) + C_M(\mathbf{s}_1, \mathbf{s}_2) \quad (21)$$

and

$$C_m(\mathbf{s}_1, \mathbf{s}_2) = C_{m-1}(\mathbf{s}_1, \mathbf{s}_2) - C_{\tau_{m-1}}(\mathbf{s}_1, \mathbf{s}_2) \quad (m = 1, \dots, M). \quad (22)$$

By substituting (22) into (21) recursively, the assertion is obtained. \square

Appendix C Derivation of Algorithms 3 and 4

C.1 Expansion of the inversion and determinant

The following lemma is used when deriving Algorithms 3 and 4.

Lemma C.1. Suppose that the assumption of Proposition 1 holds.

(a) Σ_{j_1, \dots, j_m} is positive definite for $m = 0, \dots, M$.

(b) For $m = 0, \dots, M-1$,

$$\begin{aligned} \Sigma_{j_1, \dots, j_m}^{-1} &= V_{j_1, \dots, j_m}^{-1} - V_{j_1, \dots, j_m}^{-1} B_{j_1, \dots, j_m}^m \Phi_{j_1, \dots, j_m}^\top \left(\hat{K}_{j_1, \dots, j_m}^{m-1} + \Phi_{j_1, \dots, j_m} B_{j_1, \dots, j_m}^{m\top} \right. \\ &\quad \left. \times V_{j_1, \dots, j_m}^{-1} B_{j_1, \dots, j_m}^m \Phi_{j_1, \dots, j_m}^\top \right)^{-1} \Phi_{j_1, \dots, j_m} B_{j_1, \dots, j_m}^{m\top} V_{j_1, \dots, j_m}^{-1}, \\ \det(\Sigma_{j_1, \dots, j_m}) &= \det \left(\hat{K}_{j_1, \dots, j_m}^{m-1} + \Phi_{j_1, \dots, j_m} B_{j_1, \dots, j_m}^{m\top} V_{j_1, \dots, j_m}^{-1} B_{j_1, \dots, j_m}^m \Phi_{j_1, \dots, j_m}^\top \right) \\ &\quad \times \det \left(\hat{K}_{j_1, \dots, j_m}^m \right) \det(V_{j_1, \dots, j_m}). \end{aligned}$$

Proof of Lemma C.1. (a) For $m = M$, $\Sigma_{j_1, \dots, j_M} = K_{j_1, \dots, j_M}^M \circ T_\gamma(S_{j_1, \dots, j_M}, S_{j_1, \dots, j_M}) + \tau^2 \mathbf{I}_{|S_{j_1, \dots, j_M}|}$ is positive definite from the proof of Proposition 1 (c). For $m = l+1$, assume that $\Sigma_{j_1, \dots, j_{l+1}}$ is positive definite. For $m = l$, V_{j_1, \dots, j_l} is positive definite from the definition of V_{j_1, \dots, j_l} . Additionally, from Proposition 1 (b), $\widehat{K}_{j_1, \dots, j_l}^l$ is positive definite. Thus, Σ_{j_1, \dots, j_l} is positive definite. The proof is completed by mathematical induction.

(b) From the proof of Lemma C.1 (a), V_{j_1, \dots, j_m} , $\widehat{K}_{j_1, \dots, j_m}^m$, and $\widehat{K}_{j_1, \dots, j_m}^{m-1} + \Phi_{j_1, \dots, j_m} B_{j_1, \dots, j_m}^{m\top} \times V_{j_1, \dots, j_m}^{-1} B_{j_1, \dots, j_m}^m \Phi_{j_1, \dots, j_m}^\top$ are positive definite for $m = 0, \dots, M-1$. From Theorems 18.1.1 and 18.2.8 of Harville (1997), the assertion is obtained. \square

C.2 Derivation of Algorithm 3

From (3), (4), and (5), for $1 \leq k \leq m$, $m = 1, \dots, M$, we obtain

$$\begin{aligned} K_{j_1, \dots, j_m}^k &= C_k(Q_{j_1, \dots, j_k}, Q_{j_1, \dots, j_m}) \\ &= C_{k-1}(Q_{j_1, \dots, j_k}, Q_{j_1, \dots, j_m}) - K_{j_1, \dots, j_k}^{k-1\top} \Phi_{j_1, \dots, j_{k-1}}^\top \widehat{K}_{j_1, \dots, j_{k-1}}^{k-1} \Phi_{j_1, \dots, j_{k-1}} K_{j_1, \dots, j_m}^{k-1}. \end{aligned} \quad (23)$$

By applying (3) and (4) to (23) recursively, (10) is obtained.

Next, we define $A_{j_1, \dots, j_m}^{k,l} = B_{j_1, \dots, j_m}^{k\top} V_{j_1, \dots, j_m}^{-1} B_{j_1, \dots, j_m}^l$ ($0 \leq k \leq l \leq m$, $m = 0, \dots, M-1$), $A_{j_1, \dots, j_m}^{l,k} = A_{j_1, \dots, j_m}^{k,l\top}$, and $\widetilde{A}_{j_1, \dots, j_m}^{k,l} = B_{j_1, \dots, j_m}^{k\top} \Sigma_{j_1, \dots, j_m}^{-1} B_{j_1, \dots, j_m}^l$ ($0 \leq k \leq l < m$, $m = 1, \dots, M$). Since $B_{j_1, \dots, j_m}^k = (B_{j_1, \dots, j_m, 1}^k, \dots, B_{j_1, \dots, j_m, J_{m+1}}^k)^\top$, we have

$$\begin{aligned} A_{j_1, \dots, j_m}^{k,l} &= \sum_{j_{m+1}=1}^{J_{m+1}} B_{j_1, \dots, j_m, j_{m+1}}^{k\top} \Sigma_{j_1, \dots, j_m, j_{m+1}}^{-1} B_{j_1, \dots, j_m, j_{m+1}}^l \\ &= \sum_{j_{m+1}=1}^{J_{m+1}} \widetilde{A}_{j_1, \dots, j_m, j_{m+1}}^{k,l}. \end{aligned}$$

For $m = 1, \dots, M-1$, it follows from Lemma C.1 (b) that

$$\begin{aligned} \widetilde{A}_{j_1, \dots, j_m}^{k,l} &= B_{j_1, \dots, j_m}^{k\top} V_{j_1, \dots, j_m}^{-1} B_{j_1, \dots, j_m}^l - B_{j_1, \dots, j_m}^{k\top} V_{j_1, \dots, j_m}^{-1} B_{j_1, \dots, j_m}^m \Phi_{j_1, \dots, j_m}^\top \left(\widehat{K}_{j_1, \dots, j_m}^{m-1} \right. \\ &\quad \left. + \Phi_{j_1, \dots, j_m} A_{j_1, \dots, j_m}^{m,m} \Phi_{j_1, \dots, j_m}^\top \right)^{-1} \Phi_{j_1, \dots, j_m} B_{j_1, \dots, j_m}^{m\top} V_{j_1, \dots, j_m}^{-1} B_{j_1, \dots, j_m}^l \\ &= A_{j_1, \dots, j_m}^{k,l} - A_{j_1, \dots, j_m}^{k,m} \Phi_{j_1, \dots, j_m}^\top \widehat{K}_{j_1, \dots, j_m}^m \Phi_{j_1, \dots, j_m} A_{j_1, \dots, j_m}^{m,l}. \end{aligned}$$

Thus, (11) and (12) hold.

Also, we define $\omega_{j_1, \dots, j_m}^k = B_{j_1, \dots, j_m}^{k\top} V_{j_1, \dots, j_m}^{-1} \mathbf{Z}(S_{j_1, \dots, j_m})$ ($0 \leq k \leq m$, $m = 0, \dots, M-1$) and $\widetilde{\omega}_{j_1, \dots, j_m}^k = B_{j_1, \dots, j_m}^{k\top} \Sigma_{j_1, \dots, j_m}^{-1} \mathbf{Z}(S_{j_1, \dots, j_m})$ ($0 \leq k < m$, $m = 1, \dots, M$). By the same argument as the case of $A_{j_1, \dots, j_m}^{k,l}$ and $\widetilde{A}_{j_1, \dots, j_m}^{k,l}$, we can obtain (13) and (14).

Finally, we define $d_{j_1, \dots, j_m} = \log \{ \det(\Sigma_{j_1, \dots, j_m}) \}$ and $u_{j_1, \dots, j_m} = \mathbf{Z}(S_{j_1, \dots, j_m})^\top \Sigma_{j_1, \dots, j_m}^{-1} \times \mathbf{Z}(S_{j_1, \dots, j_m})$ ($m = 0, \dots, M$). From $\Sigma_0 = C_{M\text{-RA-lp}}(S_0, S_0) + \tau^2 \mathbf{I}_n$, it follows that $d_0 =$

$\log [\det \{C_{M\text{-RA-lp}}(S_0, S_0) + \tau^2 \mathbf{I}_n\}]$ and $u_0 = \mathbf{Z}(S_0)^\top \{C_{M\text{-RA-lp}}(S_0, S_0) + \tau^2 \mathbf{I}_n\}^{-1} \mathbf{Z}(S_0)$. By using Lemma C.1 (b), for $m = 0, \dots, M-1$, we have

$$\begin{aligned}
d_{j_1, \dots, j_m} &= \log \left\{ \det \left(\widehat{K}_{j_1, \dots, j_m}^{m-1} + \Phi_{j_1, \dots, j_m} B_{j_1, \dots, j_m}^{m\top} V_{j_1, \dots, j_m}^{-1} B_{j_1, \dots, j_m}^m \Phi_{j_1, \dots, j_m}^\top \right) \right. \\
&\quad \left. \times \det \left(\widehat{K}_{j_1, \dots, j_m}^m \right) \det (V_{j_1, \dots, j_m}) \right\} \\
&= -\log \left\{ \det \left(\widetilde{K}_{j_1, \dots, j_m}^m \right) \right\} + \log \left\{ \det \left(\widehat{K}_{j_1, \dots, j_m}^m \right) \right\} + \sum_{j_{m+1}=1}^{J_{m+1}} d_{j_1, \dots, j_m, j_{m+1}}, \\
u_{j_1, \dots, j_m} &= \mathbf{Z}(S_{j_1, \dots, j_m})^\top V_{j_1, \dots, j_m}^{-1} \mathbf{Z}(S_{j_1, \dots, j_m}) - \mathbf{Z}(S_{j_1, \dots, j_m})^\top V_{j_1, \dots, j_m}^{-1} B_{j_1, \dots, j_m}^m \Phi_{j_1, \dots, j_m}^\top \\
&\quad \times \left(\widehat{K}_{j_1, \dots, j_m}^{m-1} + \Phi_{j_1, \dots, j_m} B_{j_1, \dots, j_m}^{m\top} V_{j_1, \dots, j_m}^{-1} B_{j_1, \dots, j_m}^m \Phi_{j_1, \dots, j_m}^\top \right)^{-1} \Phi_{j_1, \dots, j_m} \\
&\quad \times B_{j_1, \dots, j_m}^{m\top} V_{j_1, \dots, j_m}^{-1} \mathbf{Z}(S_{j_1, \dots, j_m}) \\
&= -\omega_{j_1, \dots, j_m}^{m\top} \Phi_{j_1, \dots, j_m}^\top \widetilde{K}_{j_1, \dots, j_m}^m \Phi_{j_1, \dots, j_m} \omega_{j_1, \dots, j_m}^m + \sum_{j_{m+1}=1}^{J_{m+1}} u_{j_1, \dots, j_m, j_{m+1}}.
\end{aligned}$$

C.3 Derivation of Algorithm 4

We will derive Algorithm 4 by an argument similar to that used in the proof of Proposition 2 in Katzfuss (2017). Let $Y_{M\text{-RA-lp}}(\mathbf{s}) \sim \text{GP}(0, C_{M\text{-RA-lp}})$ be a zero-mean Gaussian process with the degenerate covariance function $C_{M\text{-RA-lp}}$. Then, we can write

$$Y_{M\text{-RA-lp}}(\mathbf{s}) = \sum_{m=0}^{M-1} C_m(\mathbf{s}, Q^{(m)}) \Phi^{(m)\top} \boldsymbol{\eta}^{(m)} + \delta_M(\mathbf{s}),$$

where $\boldsymbol{\eta}^{(m)} = (\boldsymbol{\eta}_{1, \dots, 1}^\top, \dots, \boldsymbol{\eta}_{J_1, \dots, J_m}^\top)^\top$, $\boldsymbol{\eta}^{(0)} = \boldsymbol{\eta}_0$, $\boldsymbol{\eta}_{j_1, \dots, j_m} \sim \mathcal{N}(\mathbf{0}, \widehat{K}_{j_1, \dots, j_m}^m)$ ($m = 0, \dots, M-1$), $\delta_M(\mathbf{s}) \sim \text{GP}(0, C_M \times T_\gamma)$, and $\boldsymbol{\eta}_{j_1, \dots, j_m}$'s are independent of each other and of $\{\delta_M(\mathbf{s})\}$.

We define $\mathcal{E}_l = \{\boldsymbol{\eta}_{j_1, \dots, j_a} | 1 \leq j_1 \leq J_1, \dots, 1 \leq j_a \leq J_a, a = 0, \dots, l\}$ ($l = 0, \dots, M-1$), $\mathcal{E}_{-1} = \emptyset$, and $L_{j_1, \dots, j_M}^l = \text{Cov}(\mathbf{Y}_{M\text{-RA-lp}}(S_{j_1, \dots, j_M}^P), \mathbf{Y}_{M\text{-RA-lp}}(S_{j_1, \dots, j_l}) | \mathcal{E}_{l-1})$ ($0 \leq l \leq M$). Note that the index (j_1, \dots, j_M) is fixed. Then, for $0 \leq l < M$,

$$\begin{aligned}
L_{j_1, \dots, j_M}^l &= C_l(S_{j_1, \dots, j_M}^P, Q^{(l)}) \Phi^{(l)\top} \begin{pmatrix} \widehat{K}_{1, \dots, 1}^l & & O \\ & \ddots & \\ O & & \widehat{K}_{J_1, \dots, J_l}^l \end{pmatrix} \Phi^{(l)} C_l(S_{j_1, \dots, j_l}, Q^{(l)})^\top \\
&\quad + \text{Cov}(\mathbf{Y}_{M\text{-RA-lp}}(S_{j_1, \dots, j_M}^P), \mathbf{Y}_{M\text{-RA-lp}}(S_{j_1, \dots, j_l}) | \mathcal{E}_l). \tag{24}
\end{aligned}$$

When we define $B_{j_1, \dots, j_M}^{l,P} = C_l(S_{j_1, \dots, j_M}^P, Q_{j_1, \dots, j_l})$ for $0 \leq l \leq M$, the first term of (24) is

$$\begin{aligned}
C_l(S_{j_1, \dots, j_M}^P, Q_{j_1, \dots, j_l}) \Phi_{j_1, \dots, j_l}^\top \widehat{K}_{j_1, \dots, j_l}^l \Phi_{j_1, \dots, j_l} C_l(S_{j_1, \dots, j_l}, Q_{j_1, \dots, j_l})^\top \\
= B_{j_1, \dots, j_M}^{l,P} \Phi_{j_1, \dots, j_l}^\top \widehat{K}_{j_1, \dots, j_l}^l \Phi_{j_1, \dots, j_l} B_{j_1, \dots, j_l}^{l\top}.
\end{aligned}$$

By noting that $\text{Cov}(\mathbf{Y}_{M\text{-RA-lp}}(S_{j_1, \dots, j_M}^P), \mathbf{Y}_{M\text{-RA-lp}}(S_{j_1, \dots, j_l, j_{l+1}'})) \Big| \mathcal{E}_l = O$ for $j_{l+1}' \neq j_{l+1}$ and $\text{Cov}(\mathbf{Y}_{M\text{-RA-lp}}(S_{j_1, \dots, j_M}^P), \mathbf{Y}_{M\text{-RA-lp}}(S_{j_1, \dots, j_l, j_{l+1}})) \Big| \mathcal{E}_l = L_{j_1, \dots, j_M}^{l+1}$, the second term of (24) is expressed as

$$\begin{aligned} \text{Cov}(\mathbf{Y}_{M\text{-RA-lp}}(S_{j_1, \dots, j_M}^P), \mathbf{Y}_{M\text{-RA-lp}}(S_{j_1, \dots, j_l})) \Big| \mathcal{E}_l &= \overbrace{\left(O \quad L_{j_1, \dots, j_M}^{l+1} \quad O \right)}^{|S_{j_1, \dots, j_l}|} \\ &\quad \underbrace{\hspace{1.5cm}}_{|S_{j_1, \dots, j_l, j_{l+1}}|} \\ &= \tilde{L}_{j_1, \dots, j_M}^l, \quad (\text{say}). \end{aligned}$$

Therefore, for $0 \leq l \leq M$, we have

$$L_{j_1, \dots, j_M}^l = \begin{cases} B_{j_1, \dots, j_M}^{l,P} \Phi_{j_1, \dots, j_l}^\top \hat{K}_{j_1, \dots, j_l}^l \Phi_{j_1, \dots, j_l} B_{j_1, \dots, j_l}^{l\top} + \tilde{L}_{j_1, \dots, j_M}^l, & 0 \leq l < M, \\ C_M(S_{j_1, \dots, j_M}^P, S_{j_1, \dots, j_M}) \circ T_\gamma(S_{j_1, \dots, j_M}^P, S_{j_1, \dots, j_M}), & l = M. \end{cases} \quad (25)$$

From the definition of $\tilde{L}_{j_1, \dots, j_M}^l$,

$$\tilde{L}_{j_1, \dots, j_M}^l V_{j_1, \dots, j_l}^{-1} B_{j_1, \dots, j_l}^k = L_{j_1, \dots, j_M}^{l+1} \Sigma_{j_1, \dots, j_l, j_{l+1}}^{-1} B_{j_1, \dots, j_l, j_{l+1}}^k, \quad 0 \leq k \leq l, \quad (26)$$

$$\tilde{L}_{j_1, \dots, j_M}^l V_{j_1, \dots, j_l}^{-1} \mathbf{Z}(S_{j_1, \dots, j_l}) = L_{j_1, \dots, j_M}^{l+1} \Sigma_{j_1, \dots, j_l, j_{l+1}}^{-1} \mathbf{Z}(S_{j_1, \dots, j_l, j_{l+1}}), \quad (27)$$

$$\tilde{L}_{j_1, \dots, j_M}^l V_{j_1, \dots, j_l}^{-1} \tilde{L}_{j_1, \dots, j_M}^{l\top} = L_{j_1, \dots, j_M}^{l+1} \Sigma_{j_1, \dots, j_l, j_{l+1}}^{-1} L_{j_1, \dots, j_M}^{l+1\top}. \quad (28)$$

Now, it follows from Lemma A.2 that

$$\tilde{K}_{j_1, \dots, j_l}^l \Phi_{j_1, \dots, j_l} B_{j_1, \dots, j_l}^{l\top} V_{j_1, \dots, j_l}^{-1} = \hat{K}_{j_1, \dots, j_l}^l \Phi_{j_1, \dots, j_l} B_{j_1, \dots, j_l}^{l\top} \Sigma_{j_1, \dots, j_l}^{-1}. \quad (29)$$

Moreover, from Lemma C.1 (b) and the definition of $A_{j_1, \dots, j_M}^{k,l}$, $\Sigma_{j_1, \dots, j_l}^{-1}$ is expressed as

$$\Sigma_{j_1, \dots, j_l}^{-1} = V_{j_1, \dots, j_l}^{-1} - V_{j_1, \dots, j_l}^{-1} B_{j_1, \dots, j_l}^l \Phi_{j_1, \dots, j_l}^\top \tilde{K}_{j_1, \dots, j_l}^l \Phi_{j_1, \dots, j_l} B_{j_1, \dots, j_l}^{l\top} V_{j_1, \dots, j_l}^{-1}. \quad (30)$$

Define $\boldsymbol{\mu}_{j_1, \dots, j_M}^l = L_{j_1, \dots, j_M}^l \Sigma_{j_1, \dots, j_l}^{-1} \mathbf{Z}(S_{j_1, \dots, j_l})$ for $0 \leq l \leq M$. From the definition of L_{j_1, \dots, j_M}^l , $\boldsymbol{\mu}_{j_1, \dots, j_M}^0 = C_{M\text{-RA-lp}}(S_{j_1, \dots, j_M}^P, S_0) \{C_{M\text{-RA-lp}}(S_0, S_0) + \tau^2 \mathbf{I}_n\}^{-1} \mathbf{Z}(S_0)$. For $0 \leq l < M$, it follows from (25), (26), (27), (29), and (30) that

$$\begin{aligned} \boldsymbol{\mu}_{j_1, \dots, j_M}^l &= B_{j_1, \dots, j_M}^{l,P} \Phi_{j_1, \dots, j_l}^\top \hat{K}_{j_1, \dots, j_l}^l \Phi_{j_1, \dots, j_l} B_{j_1, \dots, j_l}^{l\top} \Sigma_{j_1, \dots, j_l}^{-1} \mathbf{Z}(S_{j_1, \dots, j_l}) \\ &\quad + \tilde{L}_{j_1, \dots, j_M}^l \Sigma_{j_1, \dots, j_l}^{-1} \mathbf{Z}(S_{j_1, \dots, j_l}) \\ &= B_{j_1, \dots, j_M}^{l,P} \Phi_{j_1, \dots, j_l}^\top \tilde{K}_{j_1, \dots, j_l}^l \Phi_{j_1, \dots, j_l} B_{j_1, \dots, j_l}^{l\top} V_{j_1, \dots, j_l}^{-1} \mathbf{Z}(S_{j_1, \dots, j_l}) \\ &\quad + \tilde{L}_{j_1, \dots, j_M}^l V_{j_1, \dots, j_l}^{-1} \mathbf{Z}(S_{j_1, \dots, j_l}) \\ &\quad - \tilde{L}_{j_1, \dots, j_M}^l V_{j_1, \dots, j_l}^{-1} B_{j_1, \dots, j_l}^l \Phi_{j_1, \dots, j_l}^\top \tilde{K}_{j_1, \dots, j_l}^l \Phi_{j_1, \dots, j_l} B_{j_1, \dots, j_l}^{l\top} V_{j_1, \dots, j_l}^{-1} \mathbf{Z}(S_{j_1, \dots, j_l}) \\ &= B_{j_1, \dots, j_M}^{l,P} \Phi_{j_1, \dots, j_l}^\top \tilde{K}_{j_1, \dots, j_l}^l \Phi_{j_1, \dots, j_l} \omega_{j_1, \dots, j_l}^l + L_{j_1, \dots, j_M}^{l+1} \Sigma_{j_1, \dots, j_{l+1}}^{-1} \mathbf{Z}(S_{j_1, \dots, j_{l+1}}) \\ &\quad - L_{j_1, \dots, j_M}^{l+1} \Sigma_{j_1, \dots, j_{l+1}}^{-1} B_{j_1, \dots, j_{l+1}}^l \Phi_{j_1, \dots, j_l}^\top \tilde{K}_{j_1, \dots, j_l}^l \Phi_{j_1, \dots, j_l} \omega_{j_1, \dots, j_l}^l \\ &= \boldsymbol{\mu}_{j_1, \dots, j_M}^{l+1} + \tilde{B}_{j_1, \dots, j_M}^{l+1,l} \Phi_{j_1, \dots, j_l}^\top \tilde{K}_{j_1, \dots, j_l}^l \Phi_{j_1, \dots, j_l} \omega_{j_1, \dots, j_l}^l, \end{aligned} \quad (31)$$

where $\tilde{B}_{j_1, \dots, j_M}^{l+1, l} = B_{j_1, \dots, j_M}^{l, P} - L_{j_1, \dots, j_M}^{l+1} \Sigma_{j_1, \dots, j_{l+1}}^{-1} B_{j_1, \dots, j_{l+1}}^l$. By applying (31) to $\boldsymbol{\mu}_{j_1, \dots, j_M}^0$ recursively, we can obtain

$$\begin{aligned} \boldsymbol{\mu}_{j_1, \dots, j_M}^0 &= L_{j_1, \dots, j_M}^M \Sigma_{j_1, \dots, j_M}^{-1} \mathbf{Z}(S_{j_1, \dots, j_M}) \\ &\quad + \sum_{k=0}^{M-1} \tilde{B}_{j_1, \dots, j_M}^{k+1, k} \Phi_{j_1, \dots, j_k}^\top \tilde{K}_{j_1, \dots, j_k}^k \Phi_{j_1, \dots, j_k} \omega_{j_1, \dots, j_k}^k. \end{aligned}$$

Next, define $V_{j_1, \dots, j_M}^{l, P} = \text{Var}(\mathbf{Y}_{M\text{-RA-lp}}(S_{j_1, \dots, j_M}^P) | \mathcal{E}_{l-1})$ for $0 \leq l \leq M$. By a derivation similar to that of (25),

$$V_{j_1, \dots, j_M}^{l, P} = \begin{cases} B_{j_1, \dots, j_M}^{l, P} \Phi_{j_1, \dots, j_l}^\top \hat{K}_{j_1, \dots, j_l}^l \Phi_{j_1, \dots, j_l} B_{j_1, \dots, j_M}^{l, P\top} + V_{j_1, \dots, j_M}^{l+1, P}, & 0 \leq l < M, \\ C_M(S_{j_1, \dots, j_M}^P, S_{j_1, \dots, j_M}^P) \circ T_\gamma(S_{j_1, \dots, j_M}^P, S_{j_1, \dots, j_M}^P), & l = M. \end{cases} \quad (32)$$

For $0 \leq l < M$, it follows from (25), (26), (28), (29), and (30) that

$$\begin{aligned} L_{j_1, \dots, j_M}^l \Sigma_{j_1, \dots, j_l}^{-1} L_{j_1, \dots, j_M}^{l\top} &= B_{j_1, \dots, j_M}^{l, P} \Phi_{j_1, \dots, j_l}^\top \hat{K}_{j_1, \dots, j_l}^l \Phi_{j_1, \dots, j_l} B_{j_1, \dots, j_M}^{l\top} \Sigma_{j_1, \dots, j_l}^{-1} B_{j_1, \dots, j_l}^l \\ &\quad \times \Phi_{j_1, \dots, j_l}^\top \hat{K}_{j_1, \dots, j_l}^l \Phi_{j_1, \dots, j_l} B_{j_1, \dots, j_M}^{l, P\top} \\ &\quad + \tilde{L}_{j_1, \dots, j_M}^l \Sigma_{j_1, \dots, j_l}^{-1} B_{j_1, \dots, j_l}^l \Phi_{j_1, \dots, j_l}^\top \hat{K}_{j_1, \dots, j_l}^l \Phi_{j_1, \dots, j_l} B_{j_1, \dots, j_M}^{l, P\top} \\ &\quad + B_{j_1, \dots, j_M}^{l, P} \Phi_{j_1, \dots, j_l}^\top \hat{K}_{j_1, \dots, j_l}^l \Phi_{j_1, \dots, j_l} B_{j_1, \dots, j_l}^\top \Sigma_{j_1, \dots, j_l}^{-1} \tilde{L}_{j_1, \dots, j_M}^{l\top} \\ &\quad + \tilde{L}_{j_1, \dots, j_M}^l \Sigma_{j_1, \dots, j_l}^{-1} \tilde{L}_{j_1, \dots, j_M}^{l\top} \\ &= B_{j_1, \dots, j_M}^{l, P} \Phi_{j_1, \dots, j_l}^\top \tilde{K}_{j_1, \dots, j_l}^l \Phi_{j_1, \dots, j_l} A_{j_1, \dots, j_l}^{l, l} \Phi_{j_1, \dots, j_l}^\top \hat{K}_{j_1, \dots, j_l}^l \\ &\quad \times \Phi_{j_1, \dots, j_l} B_{j_1, \dots, j_M}^{l, P\top} \\ &\quad + L_{j_1, \dots, j_M}^{l+1} \Sigma_{j_1, \dots, j_{l+1}}^{-1} B_{j_1, \dots, j_{l+1}}^l \Phi_{j_1, \dots, j_l}^\top \tilde{K}_{j_1, \dots, j_l}^l \Phi_{j_1, \dots, j_l} B_{j_1, \dots, j_M}^{l, P\top} \\ &\quad + B_{j_1, \dots, j_M}^{l, P} \Phi_{j_1, \dots, j_l}^\top \tilde{K}_{j_1, \dots, j_l}^l \Phi_{j_1, \dots, j_l} B_{j_1, \dots, j_{l+1}}^\top \Sigma_{j_1, \dots, j_{l+1}}^{-1} L_{j_1, \dots, j_M}^{l+1\top} \\ &\quad + L_{j_1, \dots, j_M}^{l+1} \Sigma_{j_1, \dots, j_{l+1}}^{-1} L_{j_1, \dots, j_M}^{l+1\top} \\ &\quad - L_{j_1, \dots, j_M}^{l+1} \Sigma_{j_1, \dots, j_{l+1}}^{-1} B_{j_1, \dots, j_{l+1}}^l \Phi_{j_1, \dots, j_l}^\top \tilde{K}_{j_1, \dots, j_l}^l \Phi_{j_1, \dots, j_l} \\ &\quad \times B_{j_1, \dots, j_{l+1}}^{l\top} \Sigma_{j_1, \dots, j_{l+1}}^{-1} L_{j_1, \dots, j_M}^{l+1\top} \\ &= L_{j_1, \dots, j_M}^{l+1} \Sigma_{j_1, \dots, j_{l+1}}^{-1} L_{j_1, \dots, j_M}^{l+1\top} \\ &\quad + B_{j_1, \dots, j_M}^{l, P} \Phi_{j_1, \dots, j_l}^\top \tilde{K}_{j_1, \dots, j_l}^l \Phi_{j_1, \dots, j_l} A_{j_1, \dots, j_l}^{l, l} \Phi_{j_1, \dots, j_l}^\top \hat{K}_{j_1, \dots, j_l}^l \\ &\quad \times \Phi_{j_1, \dots, j_l} B_{j_1, \dots, j_M}^{l, P\top} \\ &\quad - \tilde{B}_{j_1, \dots, j_M}^{l+1, l} \Phi_{j_1, \dots, j_l}^\top \tilde{K}_{j_1, \dots, j_l}^l \Phi_{j_1, \dots, j_l} \tilde{B}_{j_1, \dots, j_M}^{l+1, l\top} \\ &\quad + B_{j_1, \dots, j_M}^{l, P} \Phi_{j_1, \dots, j_l}^\top \tilde{K}_{j_1, \dots, j_l}^l \Phi_{j_1, \dots, j_l} B_{j_1, \dots, j_M}^{l, P\top}. \end{aligned} \quad (33)$$

Also, since $\Phi_{j_1, \dots, j_l} A_{j_1, \dots, j_l}^{l, l} \Phi_{j_1, \dots, j_l}^\top = \tilde{K}_{j_1, \dots, j_l}^{l-1} - \hat{K}_{j_1, \dots, j_l}^{l-1}$ for $0 \leq l \leq M-1$, we can show that

$$\begin{aligned} &B_{j_1, \dots, j_M}^{l, P} \Phi_{j_1, \dots, j_l}^\top \tilde{K}_{j_1, \dots, j_l}^l \Phi_{j_1, \dots, j_l} A_{j_1, \dots, j_l}^{l, l} \Phi_{j_1, \dots, j_l}^\top \hat{K}_{j_1, \dots, j_l}^l \Phi_{j_1, \dots, j_l} B_{j_1, \dots, j_M}^{l, P\top} \\ &\quad + B_{j_1, \dots, j_M}^{l, P} \Phi_{j_1, \dots, j_l}^\top \tilde{K}_{j_1, \dots, j_l}^l \Phi_{j_1, \dots, j_l} B_{j_1, \dots, j_M}^{l, P\top} \\ &= B_{j_1, \dots, j_M}^{l, P} \Phi_{j_1, \dots, j_l}^\top \hat{K}_{j_1, \dots, j_l}^l \Phi_{j_1, \dots, j_l} B_{j_1, \dots, j_M}^{l, P\top}. \end{aligned} \quad (34)$$

Now, define $\Psi_{j_1, \dots, j_M}^l = V_{j_1, \dots, j_M}^{l,P} - L_{j_1, \dots, j_M}^l \Sigma_{j_1, \dots, j_l}^{-1} L_{j_1, \dots, j_l}^{l\top}$ for $0 \leq l \leq M$. From the definition of $V_{j_1, \dots, j_M}^{l,P}$, we have

$$\begin{aligned} \Psi_{j_1, \dots, j_M}^0 &= C_{M\text{-RA-lp}}(S_{j_1, \dots, j_M}^P, S_{j_1, \dots, j_M}^P) \\ &\quad - C_{M\text{-RA-lp}}(S_{j_1, \dots, j_M}^P, S_0) \{C_{M\text{-RA-lp}}(S_0, S_0) + \tau^2 \mathbf{I}_n\}^{-1} C_{M\text{-RA-lp}}(S_{j_1, \dots, j_M}^P, S_0)^\top. \end{aligned}$$

Furthermore, from (32), (33), and (34),

$$\Psi_{j_1, \dots, j_M}^l = \Psi_{j_1, \dots, j_M}^{l+1} + \tilde{B}_{j_1, \dots, j_M}^{l+1, l} \Phi_{j_1, \dots, j_l}^\top \tilde{K}_{j_1, \dots, j_l}^l \Phi_{j_1, \dots, j_l} \tilde{B}_{j_1, \dots, j_M}^{l+1, l\top}, \quad (35)$$

for $0 \leq l < M$. Thus, by applying (35) to Ψ_{j_1, \dots, j_M}^0 recursively, it follows that

$$\begin{aligned} \Psi_{j_1, \dots, j_M}^0 &= V_{j_1, \dots, j_M}^{M,P} - L_{j_1, \dots, j_M}^M \Sigma_{j_1, \dots, j_M}^{-1} L_{j_1, \dots, j_M}^{M\top} \\ &\quad + \sum_{k=0}^{M-1} \tilde{B}_{j_1, \dots, j_M}^{k+1, k} \Phi_{j_1, \dots, j_k}^\top \tilde{K}_{j_1, \dots, j_k}^k \Phi_{j_1, \dots, j_k} \tilde{B}_{j_1, \dots, j_M}^{k+1, k\top}. \end{aligned}$$

Lastly, we will derive the calculation method of the matrices required to obtain μ_{j_1, \dots, j_M}^0 and Ψ_{j_1, \dots, j_M}^0 . We define $\tilde{B}_{j_1, \dots, j_M}^{l,k} = B_{j_1, \dots, j_M}^{k,P} - L_{j_1, \dots, j_M}^l \Sigma_{j_1, \dots, j_l}^{-1} B_{j_1, \dots, j_l}^k$ for $0 \leq k < l \leq M$. For $0 \leq k < l < M$, by using (25), (26), (29), and (30),

$$\begin{aligned} \tilde{B}_{j_1, \dots, j_M}^{l,k} &= B_{j_1, \dots, j_M}^{k,P} - B_{j_1, \dots, j_M}^{l,P} \Phi_{j_1, \dots, j_l}^\top \hat{K}_{j_1, \dots, j_l}^l \Phi_{j_1, \dots, j_l} B_{j_1, \dots, j_l}^{l\top} \Sigma_{j_1, \dots, j_l}^{-1} B_{j_1, \dots, j_l}^k \\ &\quad - \tilde{L}_{j_1, \dots, j_M}^l \Sigma_{j_1, \dots, j_l}^{-1} B_{j_1, \dots, j_l}^k \\ &= B_{j_1, \dots, j_M}^{k,P} - B_{j_1, \dots, j_M}^{l,P} \Phi_{j_1, \dots, j_l}^\top \tilde{K}_{j_1, \dots, j_l}^l \Phi_{j_1, \dots, j_l} B_{j_1, \dots, j_l}^{l\top} V_{j_1, \dots, j_l}^{-1} B_{j_1, \dots, j_l}^k \\ &\quad - \tilde{L}_{j_1, \dots, j_M}^l V_{j_1, \dots, j_l}^{-1} B_{j_1, \dots, j_l}^k \\ &\quad + \tilde{L}_{j_1, \dots, j_M}^l V_{j_1, \dots, j_l}^{-1} B_{j_1, \dots, j_l}^l \Phi_{j_1, \dots, j_l}^\top \tilde{K}_{j_1, \dots, j_l}^l \Phi_{j_1, \dots, j_l} B_{j_1, \dots, j_l}^{l\top} V_{j_1, \dots, j_l}^{-1} B_{j_1, \dots, j_l}^k \\ &= B_{j_1, \dots, j_M}^{k,P} - B_{j_1, \dots, j_M}^{l,P} \Phi_{j_1, \dots, j_l}^\top \tilde{K}_{j_1, \dots, j_l}^l \Phi_{j_1, \dots, j_l} A_{j_1, \dots, j_l}^{l,k} \\ &\quad - L_{j_1, \dots, j_M}^{l+1} \Sigma_{j_1, \dots, j_{l+1}}^{-1} B_{j_1, \dots, j_{l+1}}^k \\ &\quad + L_{j_1, \dots, j_M}^{l+1} \Sigma_{j_1, \dots, j_{l+1}}^{-1} B_{j_1, \dots, j_{l+1}}^l \Phi_{j_1, \dots, j_l}^\top \tilde{K}_{j_1, \dots, j_l}^l \Phi_{j_1, \dots, j_l} A_{j_1, \dots, j_l}^{l,k} \\ &= \tilde{B}_{j_1, \dots, j_M}^{l+1, k} - \tilde{B}_{j_1, \dots, j_M}^{l+1, l} \Phi_{j_1, \dots, j_l}^\top \tilde{K}_{j_1, \dots, j_l}^l \Phi_{j_1, \dots, j_l} A_{j_1, \dots, j_l}^{l,k}. \end{aligned}$$

Next, for $1 \leq l \leq M$, it follows from (3), (4), and (5) that

$$\begin{aligned} B_{j_1, \dots, j_M}^{l,P} &= C_l(S_{j_1, \dots, j_M}^P, Q_{j_1, \dots, j_l}) \\ &= C_{l-1}(S_{j_1, \dots, j_M}^P, Q_{j_1, \dots, j_l}) - B_{j_1, \dots, j_M}^{l-1, P} \Phi_{j_1, \dots, j_{l-1}}^\top \hat{K}_{j_1, \dots, j_{l-1}}^{l-1} \Phi_{j_1, \dots, j_{l-1}} K_{j_1, \dots, j_l}^{l-1}. \end{aligned} \quad (36)$$

By using (36) for $B_{j_1, \dots, j_M}^{l,P}$ recursively,

$$B_{j_1, \dots, j_M}^{l,P} = C_0(S_{j_1, \dots, j_M}^P, Q_{j_1, \dots, j_l}) - \sum_{k=0}^{l-1} B_{j_1, \dots, j_M}^{k,P} \Phi_{j_1, \dots, j_k}^\top \hat{K}_{j_1, \dots, j_k}^k \Phi_{j_1, \dots, j_k} K_{j_1, \dots, j_l}^k.$$

Note that $B_{j_1, \dots, j_M}^{M,P} = C_M(S_{j_1, \dots, j_M}^P, S_{j_1, \dots, j_M})$ in Step 2 of Algorithm 4 because $Q_{j_1, \dots, j_M} = S_{j_1, \dots, j_M}$. Similarly, since

$$C_M(S_{j_1, \dots, j_M}^P, S_{j_1, \dots, j_M}^P) = C_{M-1}(S_{j_1, \dots, j_M}^P, S_{j_1, \dots, j_M}^P) \\ - B_{j_1, \dots, j_M}^{M-1,P} \Phi_{j_1, \dots, j_{M-1}}^\top \hat{K}_{j_1, \dots, j_{M-1}}^{M-1} \Phi_{j_1, \dots, j_{M-1}} B_{j_1, \dots, j_M}^{M-1,P^\top}$$

from (4) and (5), we obtain

$$C_M(S_{j_1, \dots, j_M}^P, S_{j_1, \dots, j_M}^P) = C_0(S_{j_1, \dots, j_M}^P, S_{j_1, \dots, j_M}^P) \\ - \sum_{k=0}^{M-1} B_{j_1, \dots, j_M}^{k,P} \Phi_{j_1, \dots, j_k}^\top \hat{K}_{j_1, \dots, j_k}^k \Phi_{j_1, \dots, j_k} B_{j_1, \dots, j_M}^{k,P^\top}.$$

Appendix D Distributed Computing

It is assumed that we have nodes $\mathcal{N}_{j_1, \dots, j_m}$ ($m = 0, \dots, M$, $1 \leq j_1 \leq J_1, \dots, 1 \leq j_m \leq J_m$) with a tree-like structure where \mathcal{N}_0 represents a root node, and children of $\mathcal{N}_{j'_1, \dots, j'_m}$ are $\mathcal{N}_{j'_1, \dots, j'_m, i}$ ($i = 1, \dots, J_{m+1}$) for a fixed index (j'_1, \dots, j'_m) ($m = 0, \dots, M-1$). It is left to a future study to investigate how much the parallelization reduces the computational time beyond the cost of the communication.

D.1 A parallel version of Algorithm 3

The following algorithm enables us to calculate some quantities of Algorithm 3 in parallel.

Algorithm 5 (A parallel version of Algorithm 3). Given $M > 1$, D_{j_1, \dots, j_m} ($m = 1, \dots, M$, $1 \leq j_1 \leq J_1, \dots, 1 \leq j_m \leq J_m$), Q_{j_1, \dots, j_m} ($m = 0, \dots, M-1$, $1 \leq j_1 \leq J_1, \dots, 1 \leq j_{M-1} \leq J_{M-1}$), and $\gamma > 0$, find $d_0 = \log[\det\{C_{M\text{-RA-lp}}(S_0, S_0) + \tau^2 \mathbf{I}_n\}]$ and $u_0 = \mathbf{Z}(S_0)^\top \{C_{M\text{-RA-lp}}(S_0, S_0) + \tau^2 \mathbf{I}_n\}^{-1} \mathbf{Z}(S_0)$.

Step 1. Conduct Step 1 in Algorithm 3.

Step 2. In each node $\mathcal{N}_{j_1, \dots, j_M}$, calculate

$$\begin{aligned} \tilde{A}_{j_1, \dots, j_M}^{k,l} &= B_{j_1, \dots, j_M}^{k^\top} \Sigma_{j_1, \dots, j_M}^{-1} B_{j_1, \dots, j_M}^l, \quad 0 \leq k \leq l < M, \\ \tilde{\omega}_{j_1, \dots, j_M}^k &= B_{j_1, \dots, j_M}^{k^\top} \Sigma_{j_1, \dots, j_M}^{-1} \mathbf{Z}(S_{j_1, \dots, j_M}), \quad 0 \leq k < M, \\ d_{j_1, \dots, j_M} &= \log\{\det(\Sigma_{j_1, \dots, j_M})\}, \\ u_{j_1, \dots, j_M} &= \mathbf{Z}(S_{j_1, \dots, j_M})^\top \Sigma_{j_1, \dots, j_M}^{-1} \mathbf{Z}(S_{j_1, \dots, j_M}). \end{aligned}$$

Send $\tilde{A}_{j_1, \dots, j_M}^{k,l}$, $\tilde{\omega}_{j_1, \dots, j_M}^k$, d_{j_1, \dots, j_M} , and u_{j_1, \dots, j_M} to its parent, that is, $\mathcal{N}_{j_1, \dots, j_{M-1}}$.

Step 3. In each node $\mathcal{N}_{j_1, \dots, j_m}$ ($m = 1, \dots, M-1$), calculate

$$\begin{aligned}
A_{j_1, \dots, j_m}^{k,l} &= \sum_{j_{m+1}=1}^{J_{m+1}} \tilde{A}_{j_1, \dots, j_m, j_{m+1}}^{k,l}, \quad 0 \leq k \leq l \leq m, \\
\tilde{K}_{j_1, \dots, j_m}^m &= \left(\hat{K}_{j_1, \dots, j_m}^{m-1} + \Phi_{j_1, \dots, j_m} A_{j_1, \dots, j_m}^{m,m} \Phi_{j_1, \dots, j_m}^\top \right)^{-1}, \\
\tilde{A}_{j_1, \dots, j_m}^{k,l} &= A_{j_1, \dots, j_m}^{k,l} - A_{j_1, \dots, j_m}^{k,m} \Phi_{j_1, \dots, j_m}^\top \tilde{K}_{j_1, \dots, j_m}^m \Phi_{j_1, \dots, j_m} A_{j_1, \dots, j_m}^{m,l}, \quad 0 \leq k \leq l < m, \\
\omega_{j_1, \dots, j_m}^k &= \sum_{j_{m+1}=1}^{J_{m+1}} \tilde{\omega}_{j_1, \dots, j_m, j_{m+1}}^k, \quad 0 \leq k \leq m, \\
\tilde{\omega}_{j_1, \dots, j_m}^k &= \omega_{j_1, \dots, j_m}^k - A_{j_1, \dots, j_m}^{k,m} \Phi_{j_1, \dots, j_m}^\top \tilde{K}_{j_1, \dots, j_m}^m \Phi_{j_1, \dots, j_m} \omega_{j_1, \dots, j_m}^m, \quad 0 \leq k < m, \\
d_{j_1, \dots, j_m} &= -\log \left\{ \det \left(\tilde{K}_{j_1, \dots, j_m}^m \right) \right\} + \log \left\{ \det \left(\hat{K}_{j_1, \dots, j_m}^m \right) \right\} + \sum_{j_{m+1}=1}^{J_{m+1}} d_{j_1, \dots, j_m, j_{m+1}}, \\
u_{j_1, \dots, j_m} &= -\omega_{j_1, \dots, j_m}^{m^\top} \Phi_{j_1, \dots, j_m}^\top \tilde{K}_{j_1, \dots, j_m}^m \Phi_{j_1, \dots, j_m} \omega_{j_1, \dots, j_m}^m + \sum_{j_{m+1}=1}^{J_{m+1}} u_{j_1, \dots, j_m, j_{m+1}}.
\end{aligned}$$

Send $\tilde{A}_{j_1, \dots, j_m}^{k,l}$, $\tilde{\omega}_{j_1, \dots, j_m}^k$, d_{j_1, \dots, j_m} , and u_{j_1, \dots, j_m} to its parent, that is, $\mathcal{N}_{j_1, \dots, j_{m-1}}$.

Step 4. In \mathcal{N}_0 , calculate

$$\begin{aligned}
A_0^{0,0} &= \sum_{j_1=1}^{J_1} \tilde{A}_{j_1}^{0,0}, \\
\tilde{K}_0^0 &= \left(\hat{K}_0^{0-1} + \Phi_0 A_0^{0,0} \Phi_0^\top \right)^{-1}, \\
\omega_0^0 &= \sum_{j_1=1}^{J_1} \tilde{\omega}_{j_1}^0, \\
d_0 &= -\log \left\{ \det \left(\tilde{K}_0^0 \right) \right\} + \log \left\{ \det \left(\hat{K}_0^0 \right) \right\} + \sum_{j_1=1}^{J_1} d_{j_1}, \\
u_0 &= -\omega_0^{0^\top} \Phi_0^\top \tilde{K}_0^0 \Phi_0 \omega_0^0 + \sum_{j_1=1}^{J_1} u_{j_1}.
\end{aligned}$$

Step 5. Output d_0 and u_0 .

In Steps 2 and 3, the calculations at the nodes for each resolution can be conducted in parallel. Furthermore, if each node $\mathcal{N}_{j_1, \dots, j_m}$ has multiple cores, $\tilde{A}_{j_1, \dots, j_m}^{k,l}$, $\tilde{\omega}_{j_1, \dots, j_m}^k$, d_{j_1, \dots, j_m} , and u_{j_1, \dots, j_m} can also be calculated in parallel. Thus, we can conduct the efficient computation, but the communication of sending the matrices to the parent is required in Steps 2 and 3.

D.2 A parallel version of Algorithm 4

The following algorithm allows us to calculate $\boldsymbol{\mu}_{j_1, \dots, j_M}^0$ and Ψ_{j_1, \dots, j_M}^0 ($1 \leq j_1 \leq J_1, \dots, 1 \leq j_M \leq J_M$) in parallel.

Algorithm 6 (A parallel version of Algorithm 4). Given $M > 1$, D_{j_1, \dots, j_m} ($m = 1, \dots, M$, $1 \leq j_1 \leq J_1, \dots, 1 \leq j_m \leq J_m$), Q_{j_1, \dots, j_m} ($m = 0, \dots, M-1$, $1 \leq j_1 \leq J_1, \dots, 1 \leq j_{M-1} \leq J_{M-1}$), $\gamma > 0$, and S_{j_1, \dots, j_M}^P ($1 \leq j_1 \leq J_1, \dots, 1 \leq j_M \leq J_M$), find $\boldsymbol{\mu}_{j_1, \dots, j_M}^0 = C_{M\text{-RA-lp}}(S_{j_1, \dots, j_M}^P, S_0) \{C_{M\text{-RA-lp}}(S_0, S_0) + \tau^2 \mathbf{I}_n\}^{-1} \mathbf{Z}(S_0)$ and $\Psi_{j_1, \dots, j_M}^0 = C_{M\text{-RA-lp}}(S_{j_1, \dots, j_M}^P, S_{j_1, \dots, j_M}^P) - C_{M\text{-RA-lp}}(S_{j_1, \dots, j_M}^P, S_0) \{C_{M\text{-RA-lp}}(S_0, S_0) + \tau^2 \mathbf{I}_n\}^{-1} \times C_{M\text{-RA-lp}}(S_{j_1, \dots, j_M}^P, S_0)^\top$ ($1 \leq j_1 \leq J_1, \dots, 1 \leq j_M \leq J_M$).

Step 1. Conduct Step 1 in Algorithm 3.

Step 2. For the indices (j_1, \dots, j_M) ($1 \leq j_1 \leq J_1, \dots, 1 \leq j_M \leq J_M$), calculate K_{j_1, \dots, j_l}^k ($0 \leq k \leq l-1$, $1 \leq l \leq M-1$) and conduct Step 2 in Algorithm 4.

Step 3. In each node $\mathcal{N}_{j_1, \dots, j_M}$, calculate

$$\begin{aligned}\tilde{A}_{j_1, \dots, j_M}^{k,l} &= B_{j_1, \dots, j_M}^{k^\top} \Sigma_{j_1, \dots, j_M}^{-1} B_{j_1, \dots, j_M}^l, \quad 0 \leq k \leq l < M, \\ \tilde{\omega}_{j_1, \dots, j_M}^k &= B_{j_1, \dots, j_M}^{k^\top} \Sigma_{j_1, \dots, j_M}^{-1} \mathbf{Z}(S_{j_1, \dots, j_M}), \quad 0 \leq k < M, \\ \tilde{B}_{j_1, \dots, j_M}^{M,k} &= B_{j_1, \dots, j_M}^{k,P} - L_{j_1, \dots, j_M}^M \Sigma_{j_1, \dots, j_M}^{-1} B_{j_1, \dots, j_M}^k, \quad 0 \leq k < M, \\ \Psi_{j_1, \dots, j_M}^0 &= V_{j_1, \dots, j_M}^{M,P} - L_{j_1, \dots, j_M}^M \Sigma_{j_1, \dots, j_M}^{-1} L_{j_1, \dots, j_M}^{M^\top}, \\ \boldsymbol{\mu}_{j_1, \dots, j_M}^0 &= L_{j_1, \dots, j_M}^M \Sigma_{j_1, \dots, j_M}^{-1} \mathbf{Z}(S_{j_1, \dots, j_M}).\end{aligned}$$

Send $\tilde{A}_{j_1, \dots, j_M}^{k,l}$, $\tilde{\omega}_{j_1, \dots, j_M}^k$, $\tilde{B}_{j_1, \dots, j_M}^{M,k}$, Ψ_{j_1, \dots, j_M}^0 , and $\boldsymbol{\mu}_{j_1, \dots, j_M}^0$ to its parent, that is, $\mathcal{N}_{j_1, \dots, j_{M-1}}$.

Step 4. In each node $\mathcal{N}_{j_1, \dots, j_m}$ ($m = 1, \dots, M-1$), calculate

$$\begin{aligned}A_{j_1, \dots, j_m}^{k,l} &= \sum_{j_{m+1}=1}^{J_{m+1}} \tilde{A}_{j_1, \dots, j_m, j_{m+1}}^{k,l}, \quad 0 \leq k \leq l \leq m, \\ \tilde{K}_{j_1, \dots, j_m}^m &= \left(\tilde{K}_{j_1, \dots, j_m}^{m-1} + \Phi_{j_1, \dots, j_m} A_{j_1, \dots, j_m}^{m,m} \Phi_{j_1, \dots, j_m}^\top \right)^{-1}, \\ \tilde{A}_{j_1, \dots, j_m}^{k,l} &= A_{j_1, \dots, j_m}^{k,l} - A_{j_1, \dots, j_m}^{k,m} \Phi_{j_1, \dots, j_m}^\top \tilde{K}_{j_1, \dots, j_m}^m \Phi_{j_1, \dots, j_m} A_{j_1, \dots, j_m}^{m,l}, \quad 0 \leq k \leq l < m, \\ \omega_{j_1, \dots, j_m}^k &= \sum_{j_{m+1}=1}^{J_{m+1}} \tilde{\omega}_{j_1, \dots, j_m, j_{m+1}}^k, \quad 0 \leq k \leq m, \\ \tilde{\omega}_{j_1, \dots, j_m}^k &= \omega_{j_1, \dots, j_m}^k - A_{j_1, \dots, j_m}^{k,m} \Phi_{j_1, \dots, j_m}^\top \tilde{K}_{j_1, \dots, j_m}^m \Phi_{j_1, \dots, j_m} \omega_{j_1, \dots, j_m}^m, \quad 0 \leq k < m, \\ \tilde{B}_{j_1, \dots, j_m}^{m,k} &= \tilde{B}_{j_1, \dots, j_m}^{m+1,k} - \tilde{B}_{j_1, \dots, j_m}^{m+1,m} \Phi_{j_1, \dots, j_m}^\top \tilde{K}_{j_1, \dots, j_m}^m \Phi_{j_1, \dots, j_m} A_{j_1, \dots, j_m}^{m,k}, \quad 0 \leq k < m, \\ &\quad 1 \leq j_i \leq J_i, \quad i = m+1, \dots, M, \\ \Psi_{j_1, \dots, j_m}^0 &= \Psi_{j_1, \dots, j_m}^0 + \tilde{B}_{j_1, \dots, j_m}^{m+1,m} \Phi_{j_1, \dots, j_m}^\top \tilde{K}_{j_1, \dots, j_m}^m \Phi_{j_1, \dots, j_m} \tilde{B}_{j_1, \dots, j_m}^{m+1,m^\top}, \quad 1 \leq j_i \leq J_i, \\ &\quad i = m+1, \dots, M,\end{aligned}$$

$$\begin{aligned}\boldsymbol{\mu}_{j_1, \dots, j_M}^0 &= \boldsymbol{\mu}_{j_1, \dots, j_M}^0 + \tilde{B}_{j_1, \dots, j_M}^{m+1, m} \Phi_{j_1, \dots, j_m}^\top \tilde{K}_{j_1, \dots, j_m}^m \Phi_{j_1, \dots, j_m} \omega_{j_1, \dots, j_m}^m, \quad 1 \leq j_i \leq J_i, \\ &\quad i = m+1, \dots, M.\end{aligned}$$

Send $\tilde{A}_{j_1, \dots, j_m}^{k, l}$, $\tilde{\omega}_{j_1, \dots, j_m}^k$, $\tilde{B}_{j_1, \dots, j_M}^{m, k}$, Ψ_{j_1, \dots, j_M}^0 , and $\boldsymbol{\mu}_{j_1, \dots, j_M}^0$ to its parent, that is, $\mathcal{N}_{j_1, \dots, j_{m-1}}$.

Step 5. In \mathcal{N}_0 , calculate

$$\begin{aligned}A_0^{0,0} &= \sum_{j_1=1}^{J_1} \tilde{A}_{j_1}^{0,0}, \\ \tilde{K}_0^0 &= \left(\hat{K}_0^{0^{-1}} + \Phi_0 A_0^{0,0} \Phi_0^\top \right)^{-1}, \\ \omega_0^0 &= \sum_{j_1=1}^{J_1} \tilde{\omega}_{j_1}^0, \\ \Psi_{j_1, \dots, j_M}^0 &= \Psi_{j_1, \dots, j_M}^0 + \tilde{B}_{j_1, \dots, j_M}^{1,0} \Phi_0^\top \tilde{K}_0^0 \Phi_0 \tilde{B}_{j_1, \dots, j_M}^{1,0^\top}, \quad 1 \leq j_i \leq J_i, \quad i = 1, \dots, M, \\ \boldsymbol{\mu}_{j_1, \dots, j_M}^0 &= \boldsymbol{\mu}_{j_1, \dots, j_M}^0 + \tilde{B}_{j_1, \dots, j_M}^{1,0} \Phi_0^\top \tilde{K}_0^0 \Phi_0 \omega_0^0, \quad 1 \leq j_i \leq J_i, \quad i = 1, \dots, M.\end{aligned}$$

Step 6. Output $\boldsymbol{\mu}_{j_1, \dots, j_M}^0$ and Ψ_{j_1, \dots, j_M}^0 ($1 \leq j_i \leq J_i$, $i = 1, \dots, M$).

Similar to Algorithm 5, in addition to Steps 3 and 4, quantities in each node $\mathcal{N}_{j_1, \dots, j_M}$ of Step 3 can also be parallelized. Additionally, unlike Algorithm 4, Algorithm 6 can calculate $\boldsymbol{\mu}_{j_1, \dots, j_M}^0$ and Ψ_{j_1, \dots, j_M}^0 ($1 \leq j_1 \leq J_1, \dots, 1 \leq j_M \leq J_M$) in parallel. However, if the size of the prediction locations is large, the communication of sending the matrices to the parent in Steps 3 and 4 of Algorithm 6 is likely to cause a nonnegligible computational burden.

Acknowledgments

The author gratefully acknowledges the helpful comments and suggestions from the editor and two anonymous referees that refined the manuscript. This work is supported financially by JSPS KAKENHI Grant Number 18K12755.

References

- Banerjee, A., Dunson, D. B., and Tokdar, S. T. (2013). Efficient Gaussian process regression for large datasets. *Biometrika*, 100:75–89.
- Banerjee, S., Gelfand, A. E., Finley, A. O., and Sang, H. (2008). Gaussian predictive process models for large spatial data sets. *Journal of the Royal Statistical Society: Series B*, 70:825–848.

- Bevilacqua, M., Faouzi, T., Furrer, R., and Porcu, E. (2019). Estimation and prediction using generalized Wendland covariance functions under fixed domain asymptotics. *The Annals of Statistics*, 47:828–856.
- Chu, T., Zhu, J., and Wang, H. (2011). Penalized maximum likelihood estimation and variable selection in geostatistics. *The Annals of Statistics*, 39:2607–2625.
- Cressie, N. (1993). *Statistics for Spatial Data*. Wiley, New York, revised edition.
- Cressie, N. and Johannesson, G. (2008). Fixed rank kriging for very large spatial data sets. *Journal of the Royal Statistical Society: Series B*, 70:209–226.
- Cressie, N. and Wikle, C. K. (2011). *Statistics for Spatio-Temporal Data*. Wiley, Hoboken, New Jersey.
- Datta, A., Banerjee, S., Finley, A. O., and Gelfand, A. E. (2016). Hierarchical nearest-neighbor Gaussian process models for large geostatistical datasets. *Journal of the American Statistical Association*, 111:800–812.
- Dixon, J. D. (1983). Estimating extremal eigenvalues and condition numbers of matrices. *SIAM Journal on Numerical Analysis*, 20:812–814.
- Du, J., Zhang, H., and Mandrekar, V. S. (2009). Fixed-domain asymptotic properties of tapered maximum likelihood estimators. *The Annals of Statistics*, 37:3330–3361.
- Finley, A. O., Sang, H., Banerjee, S., and Gelfand, A. E. (2009). Improving the performance of predictive process modeling for large datasets. *Computational Statistics & Data Analysis*, 53:2873–2884.
- Fuentes, M. (2007). Approximate likelihood for large irregularly spaced spatial data. *Journal of the American Statistical Association*, 102:321–331.
- Furrer, R., Bachoc, F., and Du, J. (2016). Asymptotic properties of multivariate tapering for estimation and prediction. *Journal of Multivariate Analysis*, 149:177–191.
- Furrer, R., Genton, M. G., and Nychka, D. W. (2006). Covariance tapering for interpolation of large spatial datasets. *Journal of Computational and Graphical Statistics*, 15:502–523.
- Gerber, F., de Jong, R., Schaepman, M. E., Schaepman-Strub, G., and Furrer, R. (2018). Predicting missing values in spatio-temporal remote sensing data. *IEEE Transactions on Geoscience and Remote Sensing*, 56:2841–2853.

- Gneiting, T. (2002). Compactly supported correlation functions. *Journal of Multivariate Analysis*, 83:493–508.
- Gneiting, T. and Katzfuss, M. (2014). Probabilistic forecasting. *Annual Review of Statistics and Its Application*, 1:125–151.
- Gneiting, T. and Raftery, A. E. (2007). Strictly proper scoring rules, prediction, and estimation. *Journal of the American Statistical Association*, 102:359–378.
- Golub, G. H. and Van Loan, C. F. (2012). *Matrix Computations*. The Johns Hopkins University Press, Baltimore, fourth edition.
- Gramacy, R. B. and Apley, D. W. (2015). Local Gaussian process approximation for large computer experiments. *Journal of Computational and Graphical Statistics*, 24:561–578.
- Guhaniyogi, R. and Banerjee, S. (2018). Meta-kriging: Scalable Bayesian modeling and inference for massive spatial datasets. *Technometrics*, 60:430–444.
- Guinness, J. (2019). Spectral density estimation for random fields via periodic embeddings. *Biometrika*, 106:267–286.
- Halko, N., Martinsson, P. G., and Tropp, J. A. (2011). Finding structure with randomness: Probabilistic algorithms for constructing approximate matrix decompositions. *SIAM Review*, 53:217–288.
- Harville, D. A. (1997). *Matrix Algebra from a Statistician’s Perspective*. Springer, New York.
- Heaton, M. J., Datta, A., Finley, A. O., Furrer, R., Guinness, J., Guhaniyogi, R., Gerber, F., Gramacy, R. B., Hammerling, D., Katzfuss, M., Lindgren, F., Nychka, D. W., Sun, F., and Zammit-Mangion, A. (2019). A case study competition among methods for analyzing large spatial data. *Journal of Agricultural, Biological, and Environmental Statistics*, 24:398–425.
- Hirano, T. (2017). Modified linear projection for large spatial datasets. *Communications in Statistics - Simulation and Computation*, 46:870–889.
- Hirano, T. and Yajima, Y. (2013). Covariance tapering for prediction of large spatial data sets in transformed random fields. *Annals of the Institute of Statistical Mathematics*, 65:913–939.
- Horn, R. A. and Johnson, C. R. (1991). *Topics in Matrix Analysis*. Cambridge University Press.

- Jurek, M. and Katzfuss, M. (2019). Multi-resolution filters for massive spatio-temporal data. arXiv:1810.04200v2.
- Katzfuss, M. (2017). A multi-resolution approximation for massive spatial datasets. *Journal of the American Statistical Association*, 112:201–214.
- Katzfuss, M. and Gong, W. (2019). A class of multi-resolution approximations for large spatial datasets. To appear in *Statistica Sinica*.
- Katzfuss, M. and Guinness, J. (2020). A general framework for Vecchia approximations of Gaussian processes. To appear in *Statistical Science*.
- Katzfuss, M., Guinness, J., Gong, W., and Zilber, D. (2020a). Vecchia approximations of Gaussian-process predictions. To appear in *Journal of Agricultural, Biological and Environmental Statistics*.
- Katzfuss, M., Guinness, J., and Lawrence, E. (2020b). Scaled Vecchia approximation for fast computer-model emulation. arXiv:2005.00386v2.
- Kaufman, C. G., Schervish, M. J., and Nychka, D. W. (2008). Covariance tapering for likelihood-based estimation in large spatial data sets. *Journal of the American Statistical Association*, 103:1545–1555.
- Lindgren, F., Rue, H., and Lindström, J. (2011). An explicit link between Gaussian fields and Gaussian Markov random fields: The SPDE approach (with discussion). *Journal of the Royal Statistical Society: Series B*, 73:423–498.
- Liu, H., Ong, Y.-S., Shen, X., and Cai, J. (2020). When Gaussian process meets big data: A review of scalable GPs. *IEEE Transactions on Neural Networks and Learning Systems*, pages 1–19.
- Matsuda, Y. and Yajima, Y. (2009). Fourier analysis of irregularly spaced data on R^d . *Journal of the Royal Statistical Society: Series B*, 71:191–217.
- Matsuda, Y. and Yajima, Y. (2018). Locally stationary spatio-temporal processes. *Japanese Journal of Statistics and Data Science*, 1:41–57.
- Nychka, D. W., Bandyopadhyay, S., Hammerling, D., Lindgren, F., and Sain, S. (2015). A multiresolution gaussian process model for the analysis of large spatial datasets. *Journal of Computational and Graphical Statistics*, 24:579–599.
- Puntanen, S., Styan, G. P. H., and Isotalo, J. (2011). *Matrix Tricks for Linear Statistical Models: Our Personal Top Twenty*. Springer, Heidelberg.

- Sang, H. and Huang, J. Z. (2012). A full scale approximation of covariance functions for large spatial data sets. *Journal of the Royal Statistical Society: Series B*, 74:111–132.
- Stein, M. L. (2013). Statistical properties of covariance tapers. *Journal of Computational and Graphical Statistics*, 22:866–885.
- Stein, M. L., Chi, Z., and Welty, L. J. (2004). Approximating likelihoods for large spatial data sets. *Journal of the Royal Statistical Society: Series B*, 66:275–296.
- Stewart, G. W. (1993). On the early history of the singular value decomposition. *SIAM Review*, 35:551–566.
- Vecchia, A. V. (1988). Estimation and model identification for continuous spatial processes. *Journal of the Royal Statistical Society: Series B*, 50:297–312.
- Wang, D. and Loh, W.-L. (2011). On fixed-domain asymptotics and covariance tapering in Gaussian random field models. *Electronic Journal of Statistics*, 5:238–269.
- Welling, M. (2010). The kalman filter. Lecture Note.
- Wendland, H. (1995). Piecewise polynomial, positive definite and compactly supported radial functions of minimal degree. *Advances in Computational Mathematics*, 4:389–396.
- Zilber, D. and Katzfuss, M. (2020). Vecchia-Laplace approximations of generalized Gaussian processes for big non-Gaussian spatial data. arXiv:1906.07828v4.